# CARBON CAPTURE IN FIXED BED COLUMN USING COCONUT SHELL AS AN ADSORBENT

**BY**

**AKHADE DANIEL EWEAI**

**ENG2002008**

**A PROJECT SUBMITTED TO THE DEPARTMENT OF CHEMICAL ENGINEERING, UNIVERSITY OF BENIN, BENIN CITY, NIGERIA**

**IN PARTIAL FULFILMENT OF THE REQUIREMENTS FOT THE AWARD OF BACHELOR OF ENGNEERING IN CHEMICAL**

**OCTOBER, 2025**

# CERTIFICATION

This is to certify that this research project was carried out by AKHADE DANIEL EWEAI with matriculation number ENG2002008 in the Department of Chemical Engineering, University of Benin, Benin City, Edo State Nigeria.

---------- ----------

ENGR. Mrs. O. Edokpayi Date

**Project Supervisor**

---------- ----------

Engr. Prof. S.E. Uwadiae Date

**Project Coordinator**

---------- ----------

Engr. Prof. (Mrs) E.A. OYEDOH Date

**Head of Department**

---------- ----------

**External Examiner** Date

# DEDICATION

This project is dedicated to ALMIGHTY GOD, to my mother, Mrs. RITA AKANDE, whose strength and prayers have carried me through, and in the loving memory of my dear father, Mr. FRANKLIN AKHADE.

I am profoundly grateful to my uncle, Pastor. PATRICK AKADE, for his steadfast support—financially, spiritually, and morally and to my lecturers Engr. Edokpayi, Prof. Kessington, Prof. Andrew and Prof. Akhiero for their efforts.

# ACKNOWLEDGEMENT

I would like to express my heartfelt gratitude to my project supervisor, ENGR. MRS. EDOKPAYI, for her invaluable assistance, unwavering support, and timely corrections throughout this project.

I am also deeply appreciative of the Head of the Department of Chemical Engineering, PROF. (MRS.) E.T. OYEDOH, for her exceptional leadership and impact.

A special thanks goes to Dr. Fred Oshomogbo, the laboratory supervisor of LUCO Chemical Laboratory, whose support has been incredibly helpful in navigating the experimental aspects of my research.

Finally, I acknowledge the support of all my course-mates & colleagues who have supported me in the pursuit of this degree.

# ABSTRACT

This study investigated the effectiveness of activated coconut shell as an adsorbent for carbon dioxide ($CO_2$) capture, with a specific emphasis on the influence of particle size and gas flow rate on the adsorption efficiency. Coconut shells were collected locally from Benin City, Nigeria, and subjected to carbonization at 400°C for one hour, followed by acid activation using 10% hydrochloric acid. The carbonized material was classified into four particle size fractions: >500 μm, 250-500 μm, 100-250 μm, and <100 μm.

Fixed-bed column adsorption experiments were conducted at ambient temperature (29±2°C) using a 500 cm-long, 21 mm-diameter glass column with a $CO_2$ flow rate of 0.5 L/min. Breakthrough curve analysis revealed that particle size significantly affected adsorption performance, with smaller particles (100-250 μm) demonstrating superior $CO_2$ capture capacity and delayed breakthrough times compared to larger particles (>500 μm). Characterization studies using Energy Dispersive X-ray Spectroscopy (EDS) confirmed the adsorbent's predominantly carbonaceous composition (90.69 atomic% carbon) with significant nitrogen content (7.81 atomic%), while Scanning Electron Microscopy (SEM) revealed a heterogeneous porous structure favorable for gas adsorption. The finest particle fraction (<100 μm) maintained near-complete $CO_2$ removal for 30 minutes before breakthrough, while the coarsest fraction (>500 μm) reached saturation at 90 minutes.

The study concludes that coconut shell-derived activated carbon represents a viable, sustainable, and cost-effective alternative for industrial $CO_2$ capture applications, with optimal performance achieved using particle sizes in the 100-250 μm range.

# TABLE OF CONTENTS

# LIST OF FIGURES



# LIST OF TABLES

# NOMENCLATURE

- ANOVA = Analysis of Variance
- ASTM = American Society for Testing and Materials

- BET = Brunauer-Emmett-Teller (surface area analysis method)
- BJH = Barrett-Joyner-Halenda (pore size analysis method)

- CCS = Carbon Capture and Storage
- CCUS = Carbon Capture, Utilization, and Storage
- CFD = Computational Fluid Dynamics
- $CO_2$ = Carbon Dioxide
- Cu-Kα = Copper K-alpha radiation

- DFT = Density Functional Theory
- DTG = Derivative Thermogravimetry

- EDS/EDX = Energy Dispersive X-ray Spectroscopy

- FTIR = Fourier Transform Infrared Spectroscopy
- FWHM = Full Width at Half Maximum

- GHG = Greenhouse Gas

- HCl = Hydrochloric Acid
- HSD = Honestly Significant Difference (Tukey's test)

- IR = Infrared
- IPCC = Intergovernmental Panel on Climate Change
- IUPAC = International Union of Pure and Applied Chemistry

- $K_2CO_3$ = Potassium Carbonate
- KBr = Potassium Bromide
- KOH = Potassium Hydroxide

- LCA = Life Cycle Assessment

- MEA = Monoethanolamine
- MOF = Metal-Organic Framework
- MSDS = Material Safety Data Sheets

- $N_2$ = Nitrogen
- $N_2O$ = Nitrous Oxide
- NaOH = Sodium Hydroxide
- NDC = Nationally Determined Contributions
- NDIR = Non-Dispersive Infrared

- $O_2$ = Oxygen

- PFD = Process Flow Diagram

- PPE = Personal Protective Equipment
- PSA = Pressure Swing Adsorption
- ppm = Parts Per Million
- pHpzc = pH Point of Zero Charge

- RSM = Response Surface Methodology

- SEM = Scanning Electron Microscopy
- STP = Standard Temperature and Pressure

- TEM = Transmission Electron Microscopy
- TSA = Temperature Swing Adsorption

- VSA = Vacuum Swing Adsorption

- XRD = X-Ray Diffraction

# CHAPTER 1

# INTRODUCTION

## 1.1 BACKGROUND OF STUDY

Carbon dioxide (CO2) is a potent greenhouse gas that contributes significantly to global warming, which in turn has widespread environmental, economic, and societal impacts. Carbon capture has emerged as an essential and efficient means of reducing CO2 emissions, a critical step in mitigating the adverse effects of climate change and transitioning to a more sustainable future. The recognition of the importance of carbon capture underscores the urgency of developing innovative and effective technologies for capturing, utilizing, and storing CO2 emissions from various sources, such as power plants and industrial facilities, as a vital component of global efforts to combat climate change and achieve carbon neutrality.(Zhang et al., 2018)

The greenhouse effect is a natural atmospheric process fundamental to regulating Earth's climate. The mechanism is initiated when incoming shortwave solar radiation penetrates the atmosphere and is absorbed by terrestrial and aquatic surfaces. This energy is subsequently re-emitted from the Earth's surface as longwave thermal infrared (IR) radiation. While much of this outgoing radiation would typically escape to space, certain atmospheric constituents known as greenhouse gases (GHGs)—primarily water vapor (H2 O), carbon dioxide (CO2 ), methane (CH4 ), and nitrous oxide (N2 O)—absorb it. These gases, which possess atmospheric lifetimes ranging from years to centuries, trap this thermal energy and re-radiate it in all directions, warming the lower atmosphere. This planetary warming resulting from the trapping of longwave

radiation is the principal mechanism of the greenhouse effect (IPCC, 2021).(Filonchyk et al., 2024)

Anthropogenic carbon dioxide ($CO_2$) emissions have profound implications not only for atmospheric chemistry but also for marine systems. The continued absorption of atmospheric $CO_2$ by the oceans drives significant physicochemical changes, including increased ocean warming, progressive acidification, sea-level rise, and the expansion of oxygen minimum zones. As established by researchers like Gattuso et al., the severity of these phenomena and their cascading effects on marine ecosystems are directly correlated with future emission trajectories. The magnitude of these impacts will be largely dictated by the extent to which global mitigation strategies are implemented compared to a business-as-usual scenario. (Gattuso et al., 2015)

Carbon Capture and Storage (CCS) is widely acknowledged as a pivotal strategy for achieving global climate change targets. Its applications are multifaceted, encompassing the decarbonization of the power and industrial sectors, and more recently, its critical role in enabling negative emission technologies through the net removal of atmospheric carbon dioxide ($CO_2$). However, a significant discrepancy exists between its recognized potential and its current operational scale. Despite its technological maturity and a broad scientific consensus on its necessity, the large-scale implementation of CCS has not yet reached the levels projected in climate mitigation roadmaps from the past decade. (Bui et al., 2018)

## 1.2 PROBLEM STATEMENT

Although activated carbon made from plentiful agricultural waste, such as coconut shells, is a promising low-cost carbon capture option, little is known about how effective it is in real-world

industrial settings. How important dynamic parameters—more especially, gas flowrate and adsorbent particle size—interact to influence $CO_2$ capture performance in a continuous flow system is a crucial knowledge gap.

Recent advancements in adsorption-based carbon capture technology have shown promising potential, though significant challenges remain in transitioning from fundamental research to practical deployment (Zentou et al., 2025). Traditional adsorbent materials often suffer from limitations including high production costs, energy-intensive regeneration processes, limited capacity, and sustainability concerns. Consequently, there is growing interest in exploring alternative adsorbent materials derived from abundant, renewable, and low-cost biomass sources that can offer comparable or superior performance while addressing economic and environmental sustainability requirements.

The sociotechnical implications of carbon capture extend beyond purely technical considerations, encompassing economic viability, social acceptance, and integration challenges within carbon-reliant industrial systems (McLaughlin et al., 2023). The development of resilient carbon capture, transport, and storage supply chains for industrial sectors requires careful optimization to balance cost-effectiveness with system reliability and performance(Gabrielli et al., 2022). These challenges highlight the critical need for innovative, cost-efficient, and scalable carbon capture solutions that can be readily deployed across diverse industrial applications.

Systematic research to determine the ideal ratio of maximizing adsorption capacity to reducing operational problems such as pressure loss is lacking. Therefore, by examining the combined impact of particle size and flowrate on the performance of coconut shell-based adsorbents, this study tackles the challenge of developing an effective and financially feasible carbon capture system, offering crucial information for expanding this sustainable technology for industrial use in places like Nigeria.

## 1.3 SIGNIFICANCE OF THE STUDY

The increasing concentration of carbon dioxide (CO2) in the atmosphere has become a critical global concern, necessitating the development of effective and sustainable carbon capture technologies. Among various CO2 mitigation strategies, adsorption-based carbon capture has emerged as a promising approach due to its operational simplicity, energy efficiency, and potential for regeneration. The utilization of agricultural waste materials, particularly coconut shells, as precursors for activated carbon production presents a dual benefit of addressing environmental pollution while creating value-added products from biomass waste. This research on carbon capture using coconut shell adsorbent holds significant importance for both scientific advancement and practical applications in climate change mitigation.

The preparation of activated carbon from biomass materials through chemical activation has been extensively studied and proven effective for producing adsorbents with high surface area and porosity. Chemical activation using agents such as potassium hydroxide has demonstrated the ability to develop well-defined porous structures suitable for gas adsorption applications (H. Zhang et al., 2008). The activation process significantly influences the physicochemical properties of the resulting activated carbon, including surface area, pore volume, and functional groups, which directly impact the CO2 adsorption capacity (Borhan et al., 2014).

The significance of this study extends to understanding the relationship between activation methods and CO2 capture performance. Recent investigations have shown that physicochemical activation of biomass-derived porous carbons can substantially enhance their CO2 adsorption capabilities by optimizing pore structure and surface chemistry. The effect of various activation parameters on the development of microporous and mesoporous structures is crucial for

maximizing adsorption efficiency, as these pore characteristics determine the accessibility and binding sites for CO2 molecules (Patel et al., 2023).

Furthermore, this research contributes to the growing body of knowledge on modifying biosorbents to improve their performance in CO2 capture from gas mixtures. Studies have demonstrated that process parameters such as temperature, particle size, flowrate and chemical treatment can significantly influence the adsorption characteristics of biomass-based materials (Nordin et al., 2025).

Understanding these operational parameters is essential for optimizing the design and performance of coconut shell-derived adsorbents for practical carbon capture applications.

The practical significance of this study lies in its potential contribution to developing cost-effective and environmentally sustainable CO2 capture solutions. Coconut shells, being abundant agricultural residues in many tropical regions, offer an economically viable and renewable feedstock for activated carbon production. By investigating the efficacy of coconut shell-derived adsorbents, this research addresses the urgent need for scalable and affordable carbon capture technologies that can be deployed in various industrial settings. The findings from this study will provide valuable insights into the operational parameters affecting adsorption performance, thereby facilitating the optimization of carbon capture systems and contributing to global efforts in reducing greenhouse gas emissions.

## 1.4 AIM AND OBJECTIVES

The primary aim of this research is to investigate the effectiveness of activated coconut shell charcoal as an adsorbent for carbon capture. The study will specifically examine how two key parameters—**particle size** and **gas flow rate**—influence the adsorption efficiency. The goal is to identify the optimal conditions for maximizing $CO_2$ removal from a gas stream.

Some of the core objectives are

1. **Create and Characterize the Adsorbent**: Using methods like Brunauer-Emmett-Teller (BET) analysis and scanning electron microscopy (SEM), create activated charcoal from coconut shells and describe its characteristics, such as surface area, pore size distribution, and surface chemistry.
2. **Assess the Impact of Particle Size:** To ascertain how the coconut shell adsorbent's $CO_2$ adsorption capacity and kinetics are impacted by changing its particle size (fine, medium, and coarse, for example). Smaller particle sizes are thought to provide more surface area for adsorption, increasing efficiency.
3. **Evaluate the Effect of Flow Rate:** To look into the connection between the performance of the adsorbent and the gas flow rate of the $CO_2$ stream. Finding a flow rate that permits enough time for the gas molecules to come into contact with the adsorbent surface in order to accomplish maximal $CO_2$ capture without appreciably lowering the throughput is the goal.
4. **Optimize Adsorption Parameters:** To determine the ideal particle size and flow rate combination that produces the best carbon capture efficiency, hence offering useful information for the possible expansion of this technology.

5. **Create a Cost-Effective Carbon Capture Method:** To show that employing a cheap, accessible biomass waste product, such as coconut shells, as a sustainable and profitable substitute for carbon capture applications is both feasible and promising.

## 1.5 SCOPE OF STUDY

The study is **limited to using coconut shells** as the sole precursor for the activated carbon adsorbent. The shells will be sourced locally and processed in-house. Other potential biomass materials or synthetic adsorbents will not be included in this research.

Variables Under Investigation

The primary focus of this research is to analyze the effects of two specific parameters:

- **Particle Size**: The study will investigate a limited range of particle sizes for the activated charcoal (e.g., fine, medium, coarse). The specific sizes will be determined during the experimental design phase, but the study will not explore a continuous spectrum of sizes.
- **Gas Flow Rate**: The experiment will be conducted at a controlled range of gas flow rates. The study will not include extreme flow rates that fall outside the typical operational range of a lab-scale fixed-bed reactor.

The research will be conducted using a **single, fixed-bed column** for all adsorption experiments. The setup will be designed to allow for the precise control of gas flow rate and temperature. The study will not include other types of reactors, such as fluidized beds or moving beds.

The effectiveness of the carbon capture will be measured by **monitoring the $CO_2$ concentration** at the inlet and outlet of the adsorption column using a gas analyzer. The key performance indicators will be adsorption capacity (mg $CO_2$/g adsorbent) and breakthrough time. Other

advanced analyses, such as detailed kinetic modeling or thermal regeneration studies of the adsorbent, will be outside the primary scope of this project.

This study aims to provide foundational data on the relationship between particle size and flow rate for carbon capture using coconut shell adsorbent. The findings will serve as a basis for future, more extensive research, but will not encompass a full-scale industrial application or comprehensive techno-economic analysis.

# CHAPTER TWO

# Literature Review

## 2.1 Introduction

Carbon capture has emerged as a critical technology in the global effort to mitigate climate change and reduce atmospheric carbon dioxide concentrations. The increasing levels of greenhouse gases, particularly CO2, have necessitated the development of innovative solutions to capture and sequester carbon emissions from various sources. Carbon capture encompasses a range of technologies designed to separate CO2 from gas streams, whether from industrial point sources or directly from the atmosphere, with the ultimate goal of preventing its release into the environment (Dey et al., 2022). These technologies represent a vital component of the comprehensive strategies required to achieve significant reductions in global carbon emissions and meet international climate targets. The evolution of carbon capture systems has progressed from traditional post-combustion capture methods to more advanced approaches including pre-combustion capture, oxy-fuel combustion, and direct air capture technologies, each offering distinct advantages depending on the application context (Peres et al., 2022).

Among the various carbon capture methodologies, adsorption-based systems have gained considerable attention due to their operational flexibility, energy efficiency, and potential for cost-effectiveness compared to conventional absorption techniques. Adsorption processes utilize solid materials with high surface areas and specific chemical properties to selectively bind CO2 molecules from gas mixtures, offering advantages such as lower regeneration energy requirements, reduced equipment corrosion, and minimal environmental impact from degraded solvents (A. Das et al., 2023).

The performance of adsorption-based carbon capture systems is fundamentally dependent on the characteristics of the adsorbent material, including its surface area, pore structure, chemical functionality, thermal stability, and regeneration capacity. Various materials have been investigated as potential adsorbents, including zeolites, metal-organic frameworks, silica-based materials, and activated carbons, each presenting unique properties that influence their suitability for specific carbon capture applications (Victor et al., 2022). The selection of appropriate adsorbent materials is critical to achieving optimal capture efficiency, selectivity, and economic viability in industrial-scale carbon capture operations (Okesola et al., 2018).

The utilization of agricultural waste materials as precursors for activated carbon production presents a sustainable and economically attractive approach to developing high-performance adsorbents for carbon capture applications.

Coconut shell, a widely available agricultural byproduct from coconut processing industries, has demonstrated significant potential as a raw material for activated carbon synthesis due to its favorable chemical composition, high carbon content, low ash content, and well-developed microporous structure upon activation. The conversion of coconut shell into activated carbon not only provides a valuable solution for waste management but also creates a cost-effective alternative to commercial activated carbons derived from non-renewable sources(Ogungbenro et

al., 2017). Agricultural waste-based adsorbents, including those derived from coconut shells, offer multiple sustainability benefits by reducing waste disposal challenges, lowering production costs, and contributing to circular economy principles through the valorization of biomass residues. The physical and chemical properties of coconut shell-derived activated carbon can be tailored through various activation methods and processing conditions to optimize its adsorption capacity and selectivity for CO2 capture (A. Das et al., 2023). This approach aligns with the growing emphasis on developing environmentally benign and economically sustainable carbon capture technologies that can be deployed at scale to address the urgent challenges of climate change while simultaneously creating value from agricultural waste streams (Peres et al., 2022).

## 2.2 Greenhouse Gases and Climate Change

Decades of research have solidified the scientific agreement that anthropogenic climate change is occurring, with greenhouse gas emissions from burning fossil fuels being the main cause of global warming. About 76% of all greenhouse gas emissions worldwide are caused by carbon dioxide ($CO_2$), making it the most significant contributor (Gattuso et al., 2015). The atmospheric concentration of $CO_2$ has risen from pre-industrial values of roughly 280 ppm to over 410 ppm in recent years, indicating an unparalleled rate of change in Earth's atmospheric composition(Lima et al., 2021).

This dramatic rise in atmospheric $CO_2$ concentrations has numerous and far-reaching effects. Sea level rise, altered precipitation patterns, a rise in the frequency of extreme weather events, and severe ecosystem disruptions are all consequences of the continuous, large rises in global average temperatures predicted by climate models(Gattuso et al., 2015). Ocean acidification, which is caused by a rise in the number of carbon dioxide molecules that are absorbed by saltwater, offers significant dangers to marine ecosystems and biodiversity(Steiger et al., 2023).

These impacts have prompted urgent calls for comprehensive mitigation strategies that address both the sources and atmospheric concentrations of greenhouse gases.

The Intergovernmental Panel on Climate Change has emphasized that limiting global warming to 1.5°C above pre-industrial levels requires rapid, far-reaching, and unprecedented changes in all aspects of society, including substantial reductions in $CO_2$ emissions (Filonchyk et al., 2024). While renewable energy deployment and energy efficiency improvements are crucial components of mitigation strategies, the continued reliance on fossil fuels in many sectors necessitates the development and implementation of carbon capture, utilization, and storage technologies (Zhao et al., 2019). This technological imperative has driven significant research and development efforts in various carbon capture approaches, with post-combustion capture receiving particular attention due to its potential for retrofitting existing industrial infrastructure.

### 2.3. Overview of Carbon Capture and Storage (CCS) Technologies

Carbon capture and storage technologies represent a suite of approaches designed to prevent $CO_2$ emissions from reaching the atmosphere by capturing them at their source and either storing them permanently or converting them into useful products. The CCS process typically involves three main stages: capture of $CO_2$ from emission sources, transportation of the captured $CO_2$, and either permanent storage in geological formations or utilization in industrial processes(Danish & Ahmad, 2018). The capture stage, which represents the focus of this research, can be implemented through several distinct technological approaches(De Witte et al., 2021).

Pre-combustion capture involves the removal of carbon from fuel before combustion occurs, typically through gasification processes that convert coal or other carbon-containing materials into synthesis gas (syngas) consisting primarily of hydrogen and carbon monoxide(Ding & Liu, 2020). The carbon monoxide is then converted to $CO_2$ through a water-gas shift reaction, after

which the $CO_2$ is separated from the hydrogen. While this approach can achieve high capture efficiencies, it requires significant modifications to existing power generation infrastructure and is primarily applicable to new installations rather than retrofits of existing facilities(Yang et al., 2010).

Oxy-combustion capture represents another approach where fuel is burned in an atmosphere of pure oxygen rather than air, resulting in a flue gas stream consisting primarily of $CO_2$ and water vapor(Bui et al., 2018). After condensation of the water vapor, a relatively pure $CO_2$ stream is obtained that requires minimal further processing for storage or utilization. However, this approach requires the energy-intensive production of pure oxygen, typically through air separation units, which significantly impacts the overall energy penalty of the process (Plaza et al., 2017). Additionally, oxy-combustion requires substantial modifications to existing combustion systems and is generally considered more suitable for new installations.

Post-combustion capture, in contrast, involves the removal of $CO_2$ from flue gas streams after combustion has occurred. This approach offers significant advantages in terms of retrofit potential, as it can be implemented as an add-on technology to existing power plants and industrial facilities without requiring major modifications to the primary combustion systems(Dubey & Arora, 2022). Post-combustion capture can be achieved through various methods including chemical absorption using solvents such as mono-ethanol-amine (MEA), physical adsorption using solid adsorbents, membrane separation, and cryogenic separation(Raza et al., 2019). Among these options, adsorption-based capture has attracted considerable attention due to its lower energy requirements for regeneration and reduced environmental impact compared to solvent-based systems.

## 2.4 Adsorption as a Post-Combustion Carbon Capture Method

Adsorption-based carbon capture represents a promising alternative to conventional solvent-based absorption systems for post-combustion $CO_2$ removal. The fundamental principle underlying adsorption processes involves the preferential accumulation of $CO_2$ molecules on the surface of solid adsorbent materials through various molecular interactions(Dehghani et al., 2021). This approach offers several advantages over liquid absorption systems, including lower regeneration energy requirements, reduced equipment corrosion, absence of solvent degradation issues, and simplified process design(Lai et al., 2021).

The adsorption process typically operates through either temperature swing adsorption (TSA) or pressure swing adsorption (PSA) cycles. In TSA systems, $CO_2$ is adsorbed at relatively low temperatures and desorbed by heating the adsorbent material, while PSA systems utilize pressure changes to drive the adsorption and desorption processes (Mozaffari Majd et al., 2022). The choice between these approaches depends on various factors including the specific adsorbent material, the composition of the flue gas stream, and the desired purity of the captured $CO_2$ (Rubin et al., 2012). Many modern systems employ hybrid approaches that combine both temperature and pressure swings to optimize capture efficiency and minimize energy requirements.

The effectiveness of adsorption-based capture systems depends critically on the properties of the adsorbent material employed. Key performance criteria include high $CO_2$ adsorption capacity, selectivity for $CO_2$ over other flue gas components such as nitrogen and water vapor, rapid adsorption and desorption kinetics, thermal and chemical stability under operating conditions, and resistance to poisoning by trace contaminants in the flue gas(Lin et al., 2024). Additionally, practical considerations such as material cost, availability, and ease of regeneration significantly influence the commercial viability of different adsorbent options(Raganati et al., 2021).

Recent advances in adsorption-based carbon capture have focused on the development of novel adsorbent materials with enhanced performance characteristics. These efforts have included the synthesis of metal-organic frameworks (MOFs) with tunable pore structures, the development of amine-functionalized sorbents that combine physisorption and chemisorption mechanisms, and the optimization of traditional materials such as activated carbons and zeolites through advanced preparation and modification techniques(Tay et al., 2009). The growing emphasis on sustainability and circular economy principles has also driven increased interest in bio-based adsorbents derived from renewable feedstocks (Z. Zhang et al., 2018).

### 2.5 Principles of Gas Adsorption

Gas adsorption phenomena are governed by molecular interactions between gas phase molecules and solid surface atoms, with the strength and nature of these interactions determining the adsorption mechanism and performance characteristics. The two primary categories of adsorption are physisorption and chemisorption, which differ fundamentally in the nature of the molecular interactions involved and their implications for adsorption capacity, selectivity, and regeneration requirements (D. Das et al., 2015). These fundamental differences have important consequences for the design and operation of $CO_2$ capture systems using activated carbon adsorbents(Guan et al., 2018).

Physisorption, also known as physical adsorption, occurs through weak van der Waals forces between adsorbate molecules and the adsorbent surface. These interactions are relatively weak, typically ranging from 5-50 kJ/mol, and are generally reversible without chemical bond formation or breaking(Dilmore & Zhang, 2018). Physisorption is characterized by rapid equilibration, multilayer adsorption potential at higher pressures, and relatively easy regeneration through mild heating or pressure reduction. The process is typically exothermic, meaning that adsorption capacity generally decreases with increasing temperature (Rogala et al., 2018). For

$CO_2$ capture applications, physisorption offers advantages in terms of energy efficiency for regeneration and long-term stability of the adsorbent material.

Chemisorption involves the formation of chemical bonds between adsorbate molecules and surface active sites, resulting in much stronger interactions typically ranging from 50-400 kJ/mol (Ania et al., 2007). This mechanism often leads to higher selectivity for specific gas molecules but requires more energy for regeneration due to the need to break chemical bonds during desorption. Chemisorption is typically characterized by monolayer adsorption, slower kinetics compared to physisorption, and potential for irreversible reactions under certain conditions (Chu, 2020). In the context of $CO_2$ capture, chemisorption can offer enhanced selectivity and capacity but may require higher regeneration temperatures and can be subject to adsorbent degradation over multiple cycles.

The relative importance of physisorption and chemisorption in $CO_2$ capture depends on several factors including the nature of the adsorbent material, surface functional groups present, temperature and pressure conditions, and the presence of other gas components (Danish & Ahmad, 2018). Many practical adsorbent systems exhibit mixed adsorption mechanisms, with both physisorption and chemisorption contributing to overall performance(Muttakin et al., 2018). Understanding these mechanisms is crucial for optimizing adsorbent design and operating conditions to achieve maximum capture efficiency while minimizing energy requirements for regeneration.

### 2.6 Common Adsorbents for $CO_2$ Capture

The selection of appropriate adsorbent materials represents a critical factor in the development of effective carbon capture systems, with various material classes offering distinct advantages and limitations for $CO_2$ adsorption applications. Zeolites have been extensively studied as $CO_2$

adsorbents due to their well-defined pore structures, high thermal stability, and tunable surface properties (D. Das et al., 2015). These crystalline aluminosilicate materials can be synthesized with specific pore sizes and surface chemistries that promote selective $CO_2$ adsorption. However, zeolites often suffer from reduced performance in the presence of water vapor, which is commonly present in flue gas streams, and may require energy-intensive regeneration processes(Guan et al., 2018).

Metal-Organic Frameworks (MOFs) represent a relatively new class of porous materials that have generated significant interest for $CO_2$ capture applications. These materials consist of metal nodes connected by organic linkers, creating highly porous structures with exceptional surface areas that can exceed 7000 $m^2/g$ (Dehghani et al., 2021). MOFs offer the advantage of tunable pore sizes and surface functionalities through careful selection of metal centers and organic linkers, allowing for optimization of $CO_2$ adsorption properties. However, MOFs often exhibit limited hydrothermal stability and high production costs, which present challenges for large-scale implementation in industrial $CO_2$ capture systems(Lai et al., 2021).

Activated carbons represent one of the most widely studied and commercially viable adsorbent materials for $CO_2$ capture due to their high surface areas, tunable pore structures, and relatively low production costs (Dilmore & Zhang, 2018). These materials are produced through the thermal treatment of carbonaceous precursors under controlled conditions, followed by activation processes that develop porosity and surface functionality. Activated carbons can be derived from various feedstocks including coal, petroleum coke, and increasingly from renewable biomass sources(Rogala et al., 2018). The versatility of activated carbon production allows for optimization of material properties for specific applications, while their chemical stability and ease of regeneration make them attractive for industrial implementation.

Amine-functionalized adsorbents represent a hybrid approach that combines the structural advantages of solid supports with the chemical reactivity of amine groups for enhanced $CO_2$ selectivity (Ania et al., 2007). These materials can be prepared by grafting amine groups onto porous supports such as silica, activated carbon, or MOFs, or by incorporating amine-containing polymers into the adsorbent structure. The amine functionality provides chemisorption sites for $CO_2$, leading to enhanced selectivity and capacity, particularly under dilute $CO_2$ conditions typical of flue gas streams(Chu, 2020). However, amine-functionalized materials may be susceptible to oxidative degradation and poisoning by sulfur compounds present in flue gases.

### 2.7 Activated Carbon: Properties and Advantages

Activated carbon materials possess a unique combination of properties that make them particularly well-suited for gas adsorption applications, including $CO_2$ capture from flue gas streams. The most distinctive characteristic of activated carbons is their highly developed porous structure, which typically consists of a complex network of micropores (< 2 nm), mesopores (2-50 nm), and macropores (> 50 nm) (Danish & Ahmad, 2018). This hierarchical pore structure provides high specific surface areas, commonly ranging from 500 to 3000 $m^2/g$, which directly correlates with adsorption capacity for gas phase molecules. The predominance of micropores is particularly important for $CO_2$ adsorption, as these small pores provide enhanced adsorption potential due to overlapping potential fields from opposing pore walls (De Witte et al., 2021).

The surface chemistry of activated carbons plays a crucial role in determining their adsorption performance and selectivity for different gas molecules. The carbon surface contains various functional groups including carboxyl, hydroxyl, carbonyl, and lactone groups, which can influence the polarity and reactivity of the material (Bui et al., 2018). These functional groups can enhance $CO_2$ adsorption through specific interactions, particularly important under low pressure conditions typical of flue gas applications. The surface chemistry can be modified

through various post-treatment methods, including oxidation, reduction, and heteroatom incorporation, allowing for fine-tuning of adsorption properties (Muttakin et al., 2018).

From an economic perspective, activated carbons offer significant advantages over many alternative adsorbent materials. The production costs are generally lower than synthetic materials such as MOFs or engineered zeolites, particularly when biomass feedstocks are utilized(Dilmore & Zhang, 2018). The widespread availability of carbonaceous precursors and the relatively simple production processes contribute to favorable economics for large-scale implementation. Additionally, activated carbons demonstrate excellent regenerability, maintaining their adsorption capacity over multiple adsorption-desorption cycles with minimal degradation(Raza et al., 2019). This longevity is crucial for the economic viability of industrial $CO_2$ capture systems, where adsorbent replacement costs must be minimized.

The thermal and chemical stability of activated carbons under typical $CO_2$ capture operating conditions represents another significant advantage. These materials can withstand the temperature fluctuations associated with thermal swing adsorption processes and are resistant to chemical degradation by most flue gas components (Dubey & Arora, 2022). The hydrophobic nature of many activated carbons also provides advantages in applications where water vapor is present in the gas stream, as competitive adsorption of water can be minimized through appropriate surface modifications. Furthermore, activated carbons are generally inert and pose minimal safety risks in industrial applications, unlike some chemical solvents used in alternative capture technologies(Zhao et al., 2019)

.

## 2.8 Biomass as a Precursor for Activated Carbon

The utilization of biomass materials as precursors for activated carbon production has gained significant attention due to both environmental and economic considerations. Biomass represents a renewable, carbon-neutral feedstock that can reduce dependence on fossil fuel-derived precursors while contributing to sustainable materials development (Lima et al., 2021). The diverse range of available biomass sources includes agricultural residues, forestry waste, energy crops, and various organic waste streams, each offering different characteristics in terms of chemical composition, lignin content, and resulting activated carbon properties (Lin et al., 2024).

The chemical composition of biomass precursors significantly influences the properties of the resulting activated carbon materials. Key compositional factors include the relative proportions of cellulose, hemicellulose, and lignin, as well as the presence of inorganic components such as silica, potassium, and other minerals(Mozaffari Majd et al., 2022). Lignin content is particularly important as it contributes to the carbon yield during pyrolysis and influences the development of porous structure during activation. Materials with higher lignin content generally produce activated carbons with better mechanical properties and higher carbon yields, while the presence of natural minerals can catalyze activation reactions and influence pore development (Steiger et al., 2023).

The sustainability benefits of biomass-derived activated carbons extend beyond their renewable nature to include contributions to waste management and circular economy principles. Many biomass precursors are waste materials that would otherwise require disposal or generate environmental burdens through decomposition or incineration(Filonchyk et al., 2024). Converting these materials into valuable activated carbon products provides an alternative waste management pathway while creating economic value from otherwise discarded materials. This

approach aligns with global sustainability goals and can contribute to reducing the overall environmental footprint of carbon capture technologies(Tay et al., 2009).

The production of activated carbon from biomass sources also offers opportunities for distributed manufacturing and rural economic development. Unlike conventional activated carbon production that typically requires large-scale centralized facilities, biomass-based production can potentially be implemented at smaller scales closer to feedstock sources (Yang et al., 2010). This distributed approach can reduce transportation costs and emissions while creating economic opportunities in agricultural regions. However, the success of such approaches depends on developing cost-effective small-scale production technologies and ensuring consistent quality control across distributed production facilities(Z. Zhang et al., 2018).

### 2.9 Agricultural Waste Valorization for Adsorbent Production

Agricultural waste valorization for adsorbent production represents a compelling intersection of waste management, sustainability, and advanced materials development. Global agricultural production generates enormous quantities of residual materials including crop husks, shells, stalks, and processing byproducts that often pose disposal challenges while representing underutilized carbon resources(Danish & Ahmad, 2018). The conversion of these materials into high-value activated carbon adsorbents provides a pathway for transforming waste streams into valuable products while addressing environmental challenges associated with both waste disposal and carbon capture (Dubey & Arora, 2022).

The diversity of agricultural waste materials offers opportunities for optimizing activated carbon properties through careful selection of precursor materials. Different agricultural residues possess varying chemical compositions, structural characteristics, and physical properties that influence the resulting activated carbon performance(De Witte et al., 2021). For example,

nutshells and fruit stones typically contain high lignin content and dense structure that can produce mechanically strong activated carbons with well-developed microporosity. Conversely, fibrous materials such as rice husks and wheat straw may produce carbons with different pore size distributions and surface characteristics(Filonchyk et al., 2024). Understanding these relationships enables strategic selection of precursor materials based on desired adsorbent properties.

The economic benefits of agricultural waste valorization extend beyond the direct value of the produced activated carbon to include reduced waste disposal costs and potential revenue streams for agricultural producers(Lima et al., 2021). Many agricultural regions currently face significant challenges in managing waste streams, with disposal costs representing a substantial economic burden. Converting these materials into activated carbon provides an alternative that can generate revenue while reducing disposal costs (Steiger et al., 2023). Additionally, the local availability of feedstocks can reduce transportation costs compared to conventional activated carbon precursors, improving the overall economics of production.

Environmental benefits of agricultural waste valorization include reduced greenhouse gas emissions from waste decomposition, decreased pressure on landfill capacity, and reduced reliance on virgin materials for activated carbon production(Lin et al., 2024). When agricultural wastes are left to decompose naturally or are burned in open fields, they release $CO_2$ and potentially methane to the atmosphere. Converting these materials into stable activated carbon products effectively sequesters carbon while creating materials that can capture additional $CO_2$ from emission sources (Zhao et al., 2019). Life cycle assessments of biomass-derived activated carbons generally show favorable environmental profiles compared to conventional production methods.

## 2.10 Coconut Shell as a Precursor for Activated Carbon

Coconut shells represent an exceptionally promising precursor material for activated carbon production due to their unique combination of chemical composition, physical structure, and global availability. As a byproduct of coconut processing industries, coconut shells are generated in substantial quantities worldwide, with global coconut production exceeding 60 million tons annually (Ania et al., 2007). The shells typically represent 15-20% of the total coconut weight, resulting in millions of tons of shell waste that requires management. This abundance provides a reliable and consistent feedstock supply for activated carbon production while addressing waste management challenges in coconut-producing regions (Plaza et al., 2017).

The chemical composition of coconut shells makes them particularly well-suited for activated carbon production. Coconut shells contain approximately 35-40% lignin, 25-30% cellulose, and 20-25% hemicellulose, with the high lignin content contributing to excellent carbon yields during pyrolysis(Bui et al., 2018). The lignin structure provides aromatic precursors that form the graphitic carbon framework, while the relatively low ash content (typically < 5%) minimizes mineral impurities that could interfere with activation processes or block pore development. The presence of natural binding agents also contributes to the mechanical strength of the resulting activated carbon, reducing attrition and dust formation during handling and operation(Rubin et al., 2012).

The physical structure of coconut shells contributes to their suitability as activated carbon precursors through their dense, hard nature and fibrous microstructure. The density of coconut shells is typically 1.1-1.4 g/cm³, significantly higher than many other biomass materials, which contributes to higher bulk density of the resulting activated carbon and improved mechanical properties(Danish & Ahmad, 2018). The fibrous structure provides natural channels and void spaces that facilitate activation agent penetration during chemical activation, promoting uniform

pore development throughout the material. This structural advantage often results in activated carbons with more uniform pore size distributions compared to those produced from less structured biomass materials(Tay et al., 2009).

Coconut shell-derived activated carbons have demonstrated superior performance characteristics compared to many other biomass-derived carbons. Studies have consistently shown that coconut shell carbons can achieve surface areas exceeding 1500 $m^2/g$ through appropriate activation processes, with predominantly microporous structures ideal for gas adsorption applications (Muttakin et al., 2018). The $CO_2$ adsorption capacities of coconut shell activated carbons have been reported to rival or exceed those of commercial activated carbons, while offering the additional benefits of renewable feedstock utilization and lower environmental impact. The global distribution of coconut production also provides opportunities for local activated carbon production in many developing regions where $CO_2$ capture technologies are increasingly needed (Yang et al., 2010).

### 2.11 Activation Methods for Coconut Shells

The activation process represents a critical step in converting coconut shell precursors into high-performance activated carbon adsorbents, with the choice of activation method significantly influencing the resulting pore structure, surface area, and adsorption properties. Activation methods are generally classified into two main categories: physical activation and chemical activation, each offering distinct advantages and producing activated carbons with different characteristics(Chu, 2020). Understanding the mechanisms and optimization of these processes is essential for maximizing the $CO_2$ adsorption performance of coconut shell-derived adsorbents (De Witte et al., 2021).

Physical activation involves the thermal treatment of carbonized coconut shell material in the presence of oxidizing gases such as steam, carbon dioxide, or air at temperatures typically ranging from 700-1000°C. The process begins with carbonization of the coconut shell material under inert atmosphere to remove volatile components and create a carbon-rich char (Dehghani et al., 2021). Subsequently, the char is exposed to the activating gas, which selectively gasifies carbon atoms to create porosity. Steam activation is most commonly employed due to its effectiveness in developing microporosity and its relatively mild nature compared to other oxidizing gases (Rogala et al., 2018). The activation process parameters, including temperature, activation time, and gas flow rate, must be carefully optimized to achieve the desired pore structure while maintaining adequate carbon yield.

Chemical activation involves the impregnation of coconut shell material with chemical activating agents prior to pyrolysis, followed by thermal treatment in inert atmosphere. Common chemical activating agents include potassium hydroxide (KOH), phosphoric acid ($H_3PO_4$), zinc chloride ($ZnCl_2$), and potassium carbonate ($K_2CO_3$) (Lai et al., 2021). KOH activation is particularly effective for developing microporosity and achieving high surface areas, with activated carbons exceeding 3000 $m^2/g$ reported under optimal conditions. The mechanism involves the formation of metallic potassium at high temperatures, which intercalates between carbon layers and creates micropores upon washing (Mozaffari Majd et al., 2022). $H_3PO_4$ activation operates through different mechanisms involving dehydration and crosslinking reactions, typically producing materials with broader pore size distributions.

The selection of activation method depends on various factors including desired pore characteristics, economic considerations, environmental impact, and intended application requirements (Dilmore & Zhang, 2018). Chemical activation generally produces higher surface areas and greater control over pore development but involves additional chemical costs and waste treatment requirements. Physical activation is often more environmentally benign and

cost-effective but may require longer processing times and result in lower surface areas(Raganati et al., 2021). Recent research has explored combination approaches that utilize both chemical and physical activation steps to optimize pore development while balancing economic and environmental considerations.

Process optimization for coconut shell activation requires careful consideration of multiple variables and their interactions. Temperature represents a critical parameter, with higher temperatures generally promoting greater pore development but also increasing carbon burn-off and reducing yield (Lin et al., 2024). Activation time must be balanced to achieve adequate pore development without excessive material loss. For chemical activation, the ratio of activating agent to precursor material significantly influences both pore development and economic viability (Rubin et al., 2012). Recent studies have employed response surface methodology and other statistical approaches to optimize these parameters and identify conditions that maximize $CO_2$ adsorption capacity while maintaining practical yields.

### 2.12 Characterization of Activated Carbon

Comprehensive characterization of activated carbon materials is essential for understanding their structure-performance relationships and optimizing their application in $CO_2$ capture systems. The characterization process involves multiple analytical techniques that provide complementary information about different aspects of the material properties, including pore structure, surface chemistry, morphology, and thermal behavior (Ania et al., 2007). This multi-technique approach is necessary because individual characterization methods provide limited information about the complex structure of activated carbon materials (D. Das et al., 2015).

Nitrogen adsorption-desorption analysis using the Brunauer-Emmett-Teller (BET) method represents the most fundamental characterization technique for determining the specific surface

area and pore structure of activated carbons. The BET analysis involves measuring nitrogen adsorption isotherms at liquid nitrogen temperature (77 K) and applying theoretical models to calculate surface area and pore size distributions (Guan et al., 2018). The BET surface area provides a measure of the total accessible surface area, while pore size distribution analysis using methods such as density functional theory (DFT) or Barrett-Joyner-Halenda (BJH) analysis reveals the contribution of different pore size ranges to the total porosity. This information is crucial for predicting $CO_2$ adsorption performance, as microporosity is particularly important for gas adsorption applications (Z. Zhang et al., 2018).

Scanning electron microscopy (SEM) and transmission electron microscopy (TEM) provide direct visualization of activated carbon morphology and structure at micro and nanoscale levels. SEM analysis reveals surface morphology, particle shape and size distribution, and the presence of external porosity, while TEM can provide information about internal pore structure and graphitic ordering(Bui et al., 2018). These techniques are particularly valuable for understanding how activation conditions influence material structure and for identifying potential improvements in preparation methods. Energy-dispersive X-ray spectroscopy (EDS) coupled with electron microscopy can also provide elemental composition information and identify the distribution of heteroatoms or impurities (Chu, 2020).

Fourier-transform infrared spectroscopy (FTIR) analysis provides crucial information about the surface functional groups present on activated carbon materials. Different functional groups exhibit characteristic vibrational frequencies that can be identified and quantified through FTIR analysis(Danish & Ahmad, 2018). This information is particularly important for understanding the surface chemistry contributions to $CO_2$ adsorption, as certain functional groups can enhance adsorption through specific interactions. FTIR analysis can also monitor changes in surface chemistry during activation processes or after exposure to different gas atmospheres, providing insights into material stability and degradation mechanisms (Dehghani et al., 2021).

Additional characterization techniques provide complementary information about activated carbon properties relevant to $CO_2$ capture applications. Thermogravimetric analysis (TGA) reveals thermal stability and decomposition behavior under different atmospheres, which is important for understanding regeneration requirements and operational temperature limits (Lai et al., 2021). X-ray diffraction (XRD) analysis provides information about crystalline structure and degree of graphitization, while Raman spectroscopy can characterize carbon structure and defect density. Elemental analysis determines the overall composition including carbon, hydrogen, nitrogen, and sulfur content, which influences both adsorption performance and environmental compatibility (Rogala et al., 2018).

### 2.13 Theoretical Framework of Adsorption

The theoretical understanding of adsorption processes provides the fundamental basis for predicting, analyzing, and optimizing $CO_2$ capture performance using activated carbon adsorbents. Adsorption theory encompasses several levels of description, from molecular-level interactions to macroscopic equilibrium and kinetic behavior, with each level providing insights crucial for system design and operation (Ania et al., 2007). The development of robust theoretical frameworks has been essential for advancing from empirical observations to predictive models that can guide adsorbent development and process optimization (Muttakin et al., 2018).

At the molecular level, adsorption occurs through various intermolecular forces including van der Waals interactions, electrostatic forces, and in some cases, chemical bonding. For $CO_2$ adsorption on activated carbon, van der Waals forces typically dominate, with the strength of these interactions depending on the molecular polarizability of $CO_2$ and the local environment within the adsorbent pores (Bui et al., 2018). The confinement effect in micropores leads to enhanced adsorption potential due to overlapping force fields from opposing pore walls, creating

an energetically favorable environment for $CO_2$ molecules. This confinement effect is particularly pronounced in pores with dimensions similar to the $CO_2$ molecular size (approximately 0.33 nm kinetic diameter) (Danish & Ahmad, 2018).

Thermodynamic principles govern the equilibrium aspects of adsorption, with the Gibbs free energy change determining the spontaneity and extent of adsorption under given conditions. The adsorption process is typically exothermic for physisorption systems, meaning that adsorption capacity decreases with increasing temperature (De Witte et al., 2021). This temperature dependence has important implications for $CO_2$ capture applications, as flue gas temperatures are typically elevated (40-60°C), requiring consideration of temperature effects in system design. The equilibrium adsorption capacity depends on the chemical potential difference between the gas phase and adsorbed phase, which is influenced by pressure, temperature, and adsorbent-adsorbate interactions (Dilmore & Zhang, 2018).

The kinetic aspects of adsorption involve the rates of mass transfer processes that control the approach to equilibrium. Several mass transfer steps occur in sequence during adsorption: external mass transfer from the bulk gas phase to the external particle surface, intraparticle diffusion through the pore network, and adsorption/desorption at active sites (Dubey & Arora, 2022). The relative importance of these steps depends on operating conditions and material properties, with intraparticle diffusion often representing the rate-limiting step for highly microporous materials like activated carbon. Understanding these kinetic limitations is crucial for designing effective $CO_2$ capture systems with appropriate residence times and mass transfer characteristics(Guan et al., 2018).

## 2.14 Adsorption Isotherms

Adsorption isotherms represent fundamental relationships that describe the equilibrium amount of adsorbate retained by an adsorbent as a function of gas phase pressure or concentration at constant temperature. These relationships provide essential information for understanding adsorption mechanisms, comparing adsorbent performance, and designing adsorption systems (Chu, 2020). For $CO_2$ capture applications, accurate isotherm data is crucial for predicting capture capacity under various operating conditions and for sizing adsorption equipment. Several theoretical and empirical isotherm models have been developed to describe different adsorption systems, with model selection depending on the specific adsorbent-adsorbate combination and operating conditions (Lai et al., 2021).

The Langmuir isotherm model represents one of the most widely applied theoretical frameworks for describing gas adsorption on solid surfaces. This model assumes monolayer adsorption on energetically homogeneous surfaces with no interactions between adsorbed molecules (Dehghani et al., 2021). The Langmuir equation takes the form $q = q_m bP/(1+bP)$, where q is the amount adsorbed, $q_m$ is the maximum adsorption capacity, b is the Langmuir constant related to adsorption affinity, and P is the gas pressure. While the assumptions underlying the Langmuir model are rarely satisfied perfectly in real systems, it often provides good fits to experimental data over limited pressure ranges and offers physically meaningful parameters for comparing different adsorbent materials (Mozaffari Majd et al., 2022).

The Freundlich isotherm model provides an empirical approach for describing adsorption on heterogeneous surfaces with varying adsorption energies. This model takes the form $q = K_x P^{(1/n)}$, where $K_x$ and n are empirical constants that reflect adsorption capacity and intensity, respectively (Raganati et al., 2021). The Freundlich model is particularly useful for describing adsorption systems that exhibit non-linear behavior over wide pressure ranges and can

accommodate the surface heterogeneity typical of activated carbon materials. The heterogeneity parameter (1/n) provides insights into the breadth of the adsorption energy distribution, with values closer to unity indicating more homogeneous surfaces(Raza et al., 2019).

The Temkin isotherm model accounts for adsorbent-adsorbate interactions by assuming that the heat of adsorption decreases linearly with surface coverage. This model takes the form $q = (RT/b_t)\ln(a_tP)$, where R is the gas constant, T is temperature, and $a_t$ and $b_t$ are Temkin constants related to equilibrium binding and heat of adsorption, respectively (Rogala et al., 2018). The Temkin model is particularly relevant for systems where lateral interactions between adsorbed molecules are significant and can provide insights into the thermodynamics of the adsorption process. However, it is typically applicable only over intermediate coverage ranges and may not accurately describe behavior at very low or very high pressures(Steiger et al., 2023).

More complex isotherm models have been developed to address specific aspects of $CO_2$ adsorption behavior, including the Dubinin-Radushkevich model for micropore filling mechanisms and the Toth model for heterogeneous systems(Lin et al., 2024). The selection of appropriate isotherm models depends on the specific adsorbent system, operating conditions, and intended application of the data. Multi-site models and temperature-dependent isotherms are increasingly used for more accurate representation of industrial conditions(Yang et al., 2010). Recent advances in molecular simulation techniques have also enabled the development of theoretically-based isotherm models that can predict adsorption behavior from first principles.

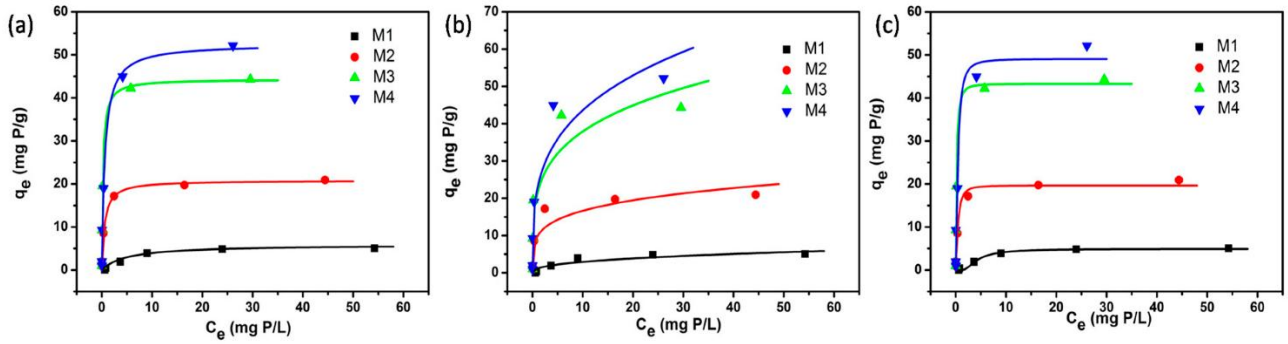


*Figure 1 Non-linear fitting of various isotherms*

*(a) Langmuir, (b) Freundlich, and (c) Dubinin-Radushkevich isotherm models for the four adsorbents (M1, M2, M3 and M4)*

## 2.15 Adsorption Kinetics

Adsorption kinetics describe the time-dependent aspects of $CO_2$ uptake by activated carbon adsorbents and are crucial for understanding mass transfer limitations and designing practical adsorption systems. The kinetic behavior determines the time required to reach equilibrium adsorption capacity and influences the sizing and operation of adsorption columns in industrial applications (D. Das et al., 2015). Several kinetic models have been developed to describe different rate-limiting mechanisms, with model selection depending on the specific system characteristics and operating conditions (Filonchyk et al., 2024).

The pseudo-first-order kinetic model, originally developed by Lagergren, assumes that the rate of adsorption is proportional to the difference between equilibrium capacity and the amount adsorbed at any time. This model takes the form $dq/dt = k_1(q_e - q)$, where $k_1$ is the pseudo-first-order rate constant and $q_e$ is the equilibrium adsorption capacity(Guan et al., 2018). The pseudo-first-order model is often applicable during the initial stages of adsorption when surface coverage is low and adsorbate-adsorbate interactions are minimal. However, it frequently fails to

describe the complete adsorption process, particularly in systems with significant intraparticle diffusion limitations (Lima et al., 2021).

The pseudo-second-order kinetic model assumes that the rate-limiting step involves chemical interactions between adsorbate and adsorbent, with the rate proportional to the square of the difference between equilibrium and instantaneous capacities. This model follows the form $dq/dt = k_2(q_e - q)^2$, where $k_2$ is the pseudo-second-order rate constant (Ding & Liu, 2020). The pseudo-second-order model often provides better fits to experimental data over the entire adsorption process and is particularly applicable to systems where chemisorption or surface complex formation occurs. The model parameters can provide insights into adsorption mechanisms and allow for comparison of different adsorbent materials (Zhao et al., 2019).

Intraparticle diffusion models are specifically designed to account for the mass transfer limitations that occur when adsorbate molecules diffuse through the internal pore network of activated carbon particles. The Weber-Morris intraparticle diffusion model relates the amount adsorbed to the square root of time, reflecting the diffusion-controlled nature of the process (Danish & Ahmad, 2018). More sophisticated models consider multiple diffusion mechanisms operating in parallel or sequence, including surface diffusion along pore walls and pore diffusion through the gas phase within pores. Understanding intraparticle diffusion is particularly important for activated carbon adsorbents due to their highly microporous nature and the potential for diffusion limitations to control overall adsorption rates (Plaza et al., 2017).

Advanced kinetic modeling approaches incorporate multiple mass transfer resistances and account for the complex pore structure of activated carbon materials. These models may consider external film diffusion, macropore diffusion, micropore diffusion, and surface reaction steps as separate resistances that contribute to overall mass transfer limitations(Tay et al., 2009). Such detailed models are essential for accurate prediction of breakthrough behavior in fixed-bed

adsorption columns and for optimization of operating conditions. The development of these models requires extensive experimental data and sophisticated parameter estimation procedures but provides more accurate predictions for industrial system design (Z. Zhang et al., 2018).

### 2.16 Breakthrough Curve Analysis in Fixed-Bed Columns

Breakthrough curve analysis represents a critical methodology for evaluating the dynamic performance of activated carbon adsorbents in continuous $CO_2$ capture applications. Unlike batch equilibrium studies that provide information about ultimate adsorption capacity, breakthrough experiments simulate the continuous operation conditions typical of industrial $CO_2$ capture systems(Bui et al., 2018). The breakthrough curve describes the outlet concentration of $CO_2$ as a function of time during continuous operation, providing information about dynamic capacity, mass transfer characteristics, and the time until adsorbent regeneration is required (Dubey & Arora, 2022).

The shape and characteristics of breakthrough curves are influenced by several factors including adsorbent properties, column design parameters, and operating conditions. A sharp breakthrough curve indicates efficient mass transfer and uniform flow distribution, while a gradual breakthrough suggests significant mass transfer limitations or flow maldistribution (De Witte et al., 2021). The breakthrough time, defined as the time when the outlet concentration reaches a specified fraction of the inlet concentration (typically 5-10%), determines the useful operating period before regeneration is required. The saturation time, when the outlet concentration approaches the inlet concentration, indicates complete saturation of the adsorbent bed (Lai et al., 2021).

Mathematical modeling of breakthrough curves provides insights into the underlying mass transfer mechanisms and allows for prediction of performance under different operating

conditions. The most commonly applied models include the Thomas model, which assumes Langmuir kinetics and plug flow behavior, the Yoon-Nelson model, which is based on the assumption that the rate of decrease in adsorption probability is proportional to the probability of adsorbate breakthrough, and the Adams-Bohart model, which describes the initial portion of the breakthrough curve (Dehghani et al., 2021). These models can be fitted to experimental data to determine kinetic parameters and predict breakthrough behavior under different conditions (Rogala et al., 2018).

The analysis of breakthrough curves provides several important performance metrics for evaluating adsorbent effectiveness in dynamic systems. The dynamic adsorption capacity, calculated from the area above the breakthrough curve, represents the actual amount of $CO_2$ captured under flowing conditions and is typically lower than the equilibrium capacity due to mass transfer limitations and incomplete utilization of the adsorbent bed (Filonchyk et al., 2024). The mass transfer zone length, which can be estimated from breakthrough curve steepness, indicates the portion of the bed that is actively adsorbing during breakthrough and influences column design requirements. These parameters are essential for scaling up laboratory results to industrial applications (Lin et al., 2024).

### 2.17 Influence of Operational Parameters on Adsorption

The performance of activated carbon adsorbents in $CO_2$ capture applications is significantly influenced by various operational parameters, with optimization of these parameters being crucial for achieving maximum capture efficiency while minimizing energy costs and operational complexity. The primary operational parameters include adsorbent particle size, gas flow rate, temperature, pressure, and gas composition, each affecting different aspects of the adsorption process through distinct mechanisms (Ania et al., 2007). Understanding these effects

and their interactions is essential for developing effective $CO_2$ capture systems and scaling laboratory results to industrial applications (Muttakin et al., 2018).

The interdependence of operational parameters creates complex optimization challenges that require systematic investigation of parameter effects and their interactions. Individual parameter optimization may not yield globally optimal conditions due to competing effects and trade-offs between different performance criteria (Danish & Ahmad, 2018). For example, increasing temperature may improve mass transfer rates but reduce equilibrium adsorption capacity, while decreasing particle size may enhance mass transfer but increase pressure drop across the adsorbent bed. These trade-offs necessitate multi-objective optimization approaches that consider all relevant performance criteria simultaneously (Tay et al., 2009).

Statistical experimental design methods, including factorial designs and response surface methodology, have proven valuable for systematically investigating parameter effects and interactions in adsorption systems. These approaches allow for efficient exploration of the parameter space while minimizing the number of required experiments (Rubin et al., 2012). The resulting empirical models can identify optimal operating conditions and provide insights into the relative importance of different parameters. Such systematic approaches are particularly important for complex systems like $CO_2$ adsorption where multiple parameters interact in non-linear ways (Yang et al., 2010).

Process modeling and simulation tools provide additional capabilities for understanding parameter effects and optimizing system performance. Computational fluid dynamics (CFD) models can simulate gas flow patterns and mass transfer within adsorption columns, while detailed kinetic models can predict breakthrough behavior under various operating conditions (Plaza et al., 2017). These modeling approaches enable investigation of parameter effects that may be difficult or expensive to study experimentally and can guide the design of more effective

$CO_2$ capture systems. The validation of these models against experimental data is crucial for ensuring their reliability and applicability to industrial conditions (Z. Zhang et al., 2018).

### 2.18 Effect of Adsorbent Particle Size on $CO_2$ Capture

Carbon dioxide capture has become increasingly critical in addressing climate change and reducing greenhouse gas emissions from industrial processes. Adsorption-based $CO_2$ capture technologies have emerged as promising solutions for post-combustion applications, where the efficiency of the capture process is influenced by various operational and material parameters. Among these parameters, adsorbent particle size plays a crucial role in determining the overall performance of the adsorption system. Understanding the relationship between particle size and $CO_2$ capture efficiency is essential for optimizing industrial-scale carbon capture systems and improving their economic viability (Raganati et al., 2021).

The particle size of adsorbent materials significantly influences the adsorption process through multiple mechanisms. Smaller particle sizes generally provide larger external surface areas and shorter diffusion paths, which can enhance mass transfer rates and improve adsorption kinetics. The relationship between particle size and adsorption performance is complex, as it involves considerations of both diffusion resistance and pressure drop across the adsorption bed. Dynamic adsorption characteristics are particularly sensitive to particle size variations, with the overall performance being governed by the balance between improved mass transfer in smaller particles and practical operational constraints such as increased pressure drop (Mitra et al., 2018) .

Particle size directly affects the accessibility of adsorption sites and the rate at which adsorbate molecules can penetrate the porous structure of the adsorbent material. Research has demonstrated that particle size influences high-pressure gas adsorption behavior, with variations in particle dimensions affecting both equilibrium capacity and the rate at which adsorption

equilibrium is achieved. The internal pore structure and surface area availability change with particle size, which consequently impacts the total adsorption capacity of the material (Zou & Rezaee, 2016). For carbon-based adsorbents specifically used in post-combustion $CO_2$ capture applications, the particle size must be carefully optimized to achieve maximum performance. The selection of appropriate particle dimensions requires balancing multiple factors including adsorption capacity, mass transfer efficiency, and pressure drop considerations. Carbon-based materials offer advantages in terms of their tunable pore structures and surface chemistry, but their effectiveness is strongly dependent on proper particle size selection for the intended application (Creamer & Gao, 2016).

The particle size of adsorbents has a pronounced effect on breakthrough curve characteristics in fixed bed adsorption systems. Breakthrough analysis provides critical insights into the dynamic performance of adsorption columns, with particle size influencing both the shape of the breakthrough curve and the breakthrough time. Smaller particles typically result in sharper breakthrough curves due to reduced mass transfer resistance, while larger particles may lead to earlier breakthrough and broader mass transfer zones. The mathematical modeling of breakthrough curves must account for particle size effects to accurately predict column performance under various operating conditions (Chu, 2020). Experimental investigations have specifically highlighted the role of activated carbon particle size in $CO_2$ capture from model flue gas streams. The studies revealed that particle size significantly affects the adsorption dynamics and overall capture efficiency, with smaller particle sizes generally demonstrating improved performance in terms of $CO_2$ uptake rates. However, the relationship is not purely linear, as very small particles can lead to excessive pressure drops and channeling effects that may compromise overall system performance. The optimal particle size range must therefore be determined based on the specific characteristics of the adsorption system and operating conditions (Balsamo et al., 2013).

Optimizing adsorbent particle size requires comprehensive analysis of multiple parameters and their interactions within the adsorption system. Process optimization approaches, including regression analysis and parametric modeling, have been employed to understand how particle size interacts with other variables such as flow rate, temperature, and adsorbent bed configuration. These analytical methods enable the identification of optimal operating conditions that maximize adsorption performance while maintaining practical feasibility for industrial applications. The optimization process must consider trade-offs between enhanced adsorption kinetics achieved with smaller particles and practical constraints related to pressure drop, material handling, and system economics (Dehghani et al., 2021).

The influence of particle size extends beyond simple adsorption capacity considerations to affect the overall design of adsorption systems. The aspect ratio of heat exchangers and the geometry of adsorption beds must be coordinated with particle size selection to achieve optimal dynamic adsorption characteristics. System-level analysis reveals that particle size effects are interconnected with heat and mass transfer phenomena, requiring integrated approaches to system design and optimization. Proper coordination of these parameters enables the development of more efficient $CO_2$ capture systems that can operate effectively under industrial conditions, ultimately contributing to the advancement of carbon capture technologies for mitigating greenhouse gas emissions (Mitra et al., 2018).

## 2.19 Effect of Gas Flow Rate on Adsorption Performance

Gas flow rate represents a fundamental operational parameter that significantly influences $CO_2$ capture performance through its effects on residence time, mass transfer characteristics, and breakthrough behavior in fixed-bed adsorption systems. The flow rate determines the contact

time between the $CO_2$-containing gas stream and the adsorbent material, with longer contact times generally promoting more complete utilization of the adsorbent capacity (Bui et al., 2018). However, the relationship between flow rate and performance is complex, involving trade-offs between residence time effects and mass transfer enhancement (Danish & Ahmad, 2018).

Lower gas flow rates provide longer residence times within the adsorbent bed, allowing more time for $CO_2$ molecules to diffuse into the adsorbent particles and reach equilibrium with the available adsorption sites. This extended contact time typically results in higher dynamic adsorption capacities and later breakthrough times, as a greater fraction of the adsorbent's equilibrium capacity can be utilized before breakthrough occurs (Ding & Liu, 2020). The residence time effect is particularly important for adsorbents with significant intraparticle diffusion limitations, where sufficient time is required for $CO_2$ molecules to penetrate the internal pore structure and access adsorption sites located within micropores (Lai et al., 2021).

Conversely, higher gas flow rates can enhance external mass transfer coefficients by increasing turbulence and reducing boundary layer thickness around adsorbent particles. This enhancement in external mass transfer can be beneficial when external mass transfer resistance is significant relative to other resistances in the system (Lima et al., 2021). The relationship between flow rate and external mass transfer coefficient follows power law correlations derived from dimensionless analysis, typically showing that mass transfer coefficients increase with flow rate raised to a power between 0.5 and 0.8, depending on the specific system geometry and flow regime (Mozaffari Majd et al., 2022).

The optimization of gas flow rate must consider both performance and economic factors, as higher flow rates generally require larger equipment sizes to maintain adequate residence times and may increase pressure drop and associated energy costs. The concept of optimal flow rate depends on the specific objectives of the capture system, whether prioritizing maximum $CO_2$

recovery, minimum energy consumption, or maximum throughput (Raganati et al., 2021). Recent studies have employed multi-objective optimization approaches to identify optimal flow rate conditions that balance these competing objectives while considering practical constraints such as equipment limitations and regeneration requirements (Rogala et al., 2018).

### 2.20 Effect of Temperature on Adsorption Efficiency

Temperature represents one of the most influential operational parameters in $CO_2$ adsorption systems, with its effects operating through both thermodynamic and kinetic mechanisms. For physisorption systems typical of $CO_2$ adsorption on activated carbon, the process is inherently exothermic, meaning that equilibrium adsorption capacity decreases with increasing temperature according to thermodynamic principles (Chu, 2020). This temperature dependence has profound implications for $CO_2$ capture from flue gas streams, which are typically at elevated temperatures (40-80°C) compared to ambient conditions where many laboratory studies are conducted(De Witte et al., 2021).

The thermodynamic relationship between temperature and adsorption capacity can be quantified through the Clausius-Clapeyron equation and van't Hoff analysis, which relate the equilibrium constant to temperature through the isosteric heat of adsorption. For most activated carbon-$CO_2$ systems, the isosteric heat of adsorption ranges from 15-40 kJ/mol, indicating relatively weak physisorption interactions(Dehghani et al., 2021). This heat of adsorption determines the sensitivity of adsorption capacity to temperature changes, with higher heats of adsorption resulting in greater temperature sensitivity. Understanding this relationship is crucial for predicting performance under industrial conditions and for optimizing regeneration strategies (Dubey & Arora, 2022).

While higher temperatures generally reduce equilibrium adsorption capacity, they can simultaneously enhance adsorption kinetics by increasing molecular mobility and diffusion rates. The diffusion coefficient for gas phase molecules typically increases exponentially with temperature according to the Arrhenius relationship, leading to faster approach to equilibrium at higher temperatures(Guan et al., 2018). This enhancement in kinetics can partially offset the capacity reduction, particularly in systems where mass transfer limitations are significant. The net effect of temperature on dynamic performance depends on the relative importance of equilibrium and kinetic contributions under specific operating conditions(Raza et al., 2019).

Temperature also affects the selectivity of $CO_2$ adsorption in the presence of other gas components such as nitrogen and water vapor. The temperature dependence of selectivity arises from differences in the heats of adsorption for different gas molecules, with more strongly adsorbed species typically showing greater temperature sensitivity (Lin et al., 2024). For $CO_2/N_2$ separation, selectivity generally decreases with increasing temperature due to the higher heat of adsorption for $CO_2$ compared to $N_2$. However, temperature can be used strategically to optimize selectivity under specific conditions, and temperature swing processes exploit these relationships for efficient separation and regeneration (Steiger et al., 2023).

The practical implications of temperature effects extend to system design considerations including heat integration opportunities and regeneration strategies. The exothermic nature of $CO_2$ adsorption means that heat is released during the capture process, which must be managed to maintain optimal operating temperatures (Tay et al., 2009). Conversely, the endothermic desorption process requires heat input for regeneration, creating opportunities for heat integration between adsorption and desorption steps. Understanding temperature effects is also crucial for seasonal operation optimization, as ambient temperature variations can significantly influence system performance (Yang et al., 2010).

## 2.21 Interaction Effects Between Operational Parameters

The simultaneous influence of multiple operational parameters on $CO_2$ adsorption performance creates complex interaction effects that cannot be predicted from individual parameter studies alone. These interactions arise from the coupled nature of mass transfer, thermodynamic equilibrium, and bed hydrodynamics in real adsorption systems (Ania et al., 2007). Understanding and quantifying these interactions is essential for optimizing system performance and scaling laboratory results to industrial applications, as optimal conditions for individual parameters may not correspond to globally optimal conditions when parameters are varied simultaneously (Filonchyk et al., 2024).

The interaction between particle size and gas flow rate represents one of the most significant parameter interactions in packed bed adsorption systems. While smaller particles generally enhance mass transfer, this benefit may be offset by increased pressure drop at higher flow rates, creating an optimal combination that depends on the specific system objectives (Danish & Ahmad, 2018). The interaction manifests through the competing effects of enhanced external mass transfer and increased bed resistance, with the optimal combination depending on the relative importance of mass transfer enhancement versus pressure drop penalties. Recent studies have used response surface methodology to map these interactions and identify optimal operating regions(De Witte et al., 2021).

Temperature and flow rate interactions occur through their combined effects on mass transfer coefficients and residence time distributions within the adsorbent bed. Higher temperatures enhance diffusion rates and mass transfer coefficients but reduce equilibrium capacity, while higher flow rates provide enhanced external mass transfer but reduced residence times(Dehghani et al., 2021). The optimal combination depends on whether the system is limited by equilibrium capacity or kinetic factors, with kinetically-limited systems benefiting more from higher

temperatures despite capacity reductions. These interactions are particularly important for optimizing breakthrough curves and determining optimal cycling conditions for temperature swing processes (Lai et al., 2021).

The three-way interaction between particle size, flow rate, and temperature creates even more complex optimization landscapes that require sophisticated experimental designs and modeling approaches. These interactions may result in optimal conditions that are significantly different from those predicted by two-parameter studies or individual parameter optimization (Lima et al., 2021). For example, the optimal particle size may depend on both flow rate and temperature, with different optimal sizes for different temperature-flow rate combinations. Understanding these higher-order interactions is crucial for developing robust operating strategies that perform well under varying industrial conditions (Mozaffari Majd et al., 2022).

Statistical modeling and machine learning approaches have emerged as powerful tools for understanding and predicting parameter interactions in complex adsorption systems. These methods can identify non-linear relationships and high-order interactions that may not be apparent from traditional analysis approaches (Raganati et al., 2021). Response surface models, artificial neural networks, and other data-driven approaches can map the complex relationship between multiple operational parameters and system performance, enabling optimization under realistic industrial constraints. The integration of these modeling approaches with mechanistic understanding provides a comprehensive framework for system optimization (Zhao et al., 2019).

### 2.22 Regeneration of Spent Coconut Shell Adsorbent

The regeneration of spent coconut shell activated carbon adsorbents represents a critical aspect of $CO_2$ capture system operation, directly affecting both the economic viability and environmental sustainability of the capture process. Effective regeneration must restore the

adsorbent's $CO_2$ capture capacity while minimizing energy consumption, maintaining material stability, and preventing degradation over multiple cycles (Chu, 2020). The regeneration process typically involves desorbing captured $CO_2$ from the adsorbent surface and pore structure, producing a concentrated $CO_2$ stream suitable for compression and storage or utilization (Rogala et al., 2018).

Thermal swing adsorption (TSA) represents the most commonly employed regeneration method for activated carbon adsorbents, utilizing temperature increases to drive $CO_2$ desorption. The process typically involves heating the saturated adsorbent to temperatures ranging from 80-200°C, depending on the strength of $CO_2$-adsorbent interactions and the desired degree of regeneration (Danish & Ahmad, 2018). The heating can be accomplished through various methods including hot gas purging, steam heating, electrical heating, or microwave heating. The choice of heating method affects both the energy efficiency and the uniformity of regeneration throughout the adsorbent bed (Steiger et al., 2023). TSA processes generally achieve high degrees of regeneration but require significant energy input for heating and subsequent cooling.

Pressure swing adsorption (PSA) offers an alternative regeneration approach that utilizes pressure reduction to drive $CO_2$ desorption without requiring significant temperature changes. This method can be more energy-efficient than TSA when $CO_2$ adsorption isotherms show strong pressure dependence and when waste heat is not readily available for thermal regeneration (De Witte et al., 2021). PSA processes typically operate through vacuum swing adsorption (VSA) where pressure is reduced below atmospheric pressure, or through pressure reduction to atmospheric conditions. The energy requirements for PSA depend on the vacuum levels required and the efficiency of vacuum pumps, with recent advances in vacuum technology improving the economic attractiveness of PSA approaches (Raza et al., 2019).

Hybrid regeneration approaches that combine thermal and pressure swing elements have been developed to optimize energy efficiency and regeneration completeness. These approaches may involve simultaneous heating and pressure reduction, sequential application of thermal and pressure swings, or temperature-controlled pressure swing processes (Dehghani et al., 2021). The optimization of hybrid regeneration requires careful consideration of energy integration opportunities, such as using waste heat from other process steps or heat recovery from cooling operations. Recent research has explored innovative regeneration concepts including microwave-assisted desorption and electrically conductive adsorbents for direct electrical heating (Lin et al., 2024).

The long-term stability of coconut shell activated carbon during repeated regeneration cycles is crucial for practical implementation. Factors affecting stability include thermal degradation at high regeneration temperatures, oxidation in the presence of oxygen, mechanical attrition due to thermal cycling, and chemical changes due to exposure to flue gas contaminants (Dilmore & Zhang, 2018). Studies have investigated the performance of coconut shell adsorbents over multiple cycles, generally showing good stability with modest capacity losses over hundreds of cycles. Understanding degradation mechanisms and developing strategies to minimize them is essential for ensuring long-term system reliability and economic performance (Tay et al., 2009).

### 2.23 Previous Studies on $CO_2$ Capture Using Coconut Shell Adsorbents

Research on coconut shell-derived activated carbon for $CO_2$ capture has demonstrated the significant potential of this renewable adsorbent material, with numerous studies reporting competitive performance compared to commercial activated carbons and other adsorbent materials. Early investigations focused primarily on the development of activation methods and basic characterization of the resulting materials, while more recent studies have examined dynamic performance, operational parameter optimization, and long-term stability under realistic

operating conditions (Ania et al., 2007). The evolution of this research field has progressively moved from fundamental material development to practical application considerations (Bui et al., 2018). Several studies have investigated the optimization of activation conditions for coconut shell-derived activated carbons specifically for $CO_2$ capture applications. Research by various groups has examined both chemical and physical activation methods, with KOH activation generally producing the highest surface areas and $CO_2$ capacities(Danish & Ahmad, 2018). Optimal activation conditions typically involve KOH:char ratios of 2:1 to 4:1, activation temperatures of 700-800°C, and activation times of 1-3 hours. Under these conditions, coconut shell activated carbons have achieved BET surface areas exceeding 2000 $m^2/g$ and $CO_2$ capacities of 3-5 mmol/g at standard conditions (Muttakin et al., 2018).

Dynamic performance studies using packed bed columns have demonstrated the practical effectiveness of coconut shell activated carbons for continuous $CO_2$ capture. Breakthrough curve analyses have shown that these materials can achieve dynamic capacities representing 60-80% of their equilibrium capacities under realistic flow conditions(Dehghani et al., 2021). The breakthrough times and mass transfer characteristics have been found to be comparable to or better than commercial activated carbons, validating the potential for industrial application. Studies have also examined the effects of bed height, gas velocity, and temperature on breakthrough performance, providing design guidance for larger-scale implementations (Dubey & Arora, 2022).

Comparative studies have evaluated coconut shell activated carbons against other biomass-derived adsorbents and commercial materials, consistently showing competitive or superior performance. The comparison criteria have included equilibrium adsorption capacity, selectivity for $CO_2$ over $N_2$, regeneration efficiency, and long-term stability (Rogala et al., 2018). Coconut shell carbons have generally performed well in these comparisons, often showing advantages in terms of mechanical strength, regeneration efficiency, and cost-effectiveness. These comparative

studies have helped establish the position of coconut shell adsorbents within the broader landscape of $CO_2$ capture materials (Z. Zhang et al., 2018).

### 2.24 Research Gaps and Knowledge Deficiencies

Despite the significant progress in understanding coconut shell activated carbon for $CO_2$ capture, several important research gaps and knowledge deficiencies remain that limit the optimization and industrial implementation of these materials. One significant gap exists in the understanding of structure-performance relationships under realistic industrial conditions, as most studies have been conducted under idealized laboratory conditions that may not accurately represent the complex environment of actual flue gas streams(Chu, 2020).

Industrial flue gases contain various contaminants including sulfur compounds, nitrogen oxides, particulates, and water vapor that can significantly affect adsorbent performance through competitive adsorption, chemical reactions, or physical blocking of pores (Raganati et al., 2021).

The long-term stability and degradation mechanisms of coconut shell activated carbons under industrial operating conditions remain insufficiently understood. While short-term cycling studies have demonstrated reasonable stability, the effects of extended exposure to realistic flue gas compositions, temperature cycling, and mechanical stress over thousands of operating cycles have not been comprehensively studied (De Witte et al., 2021). Understanding these long-term effects is crucial for predicting adsorbent lifetime, optimizing replacement schedules, and ensuring reliable system operation. Additionally, the mechanisms of capacity loss and potential regeneration strategies for partially degraded adsorbents require further investigation (Steiger et al., 2023).

Limited research has been conducted on the optimization of coconut shell activated carbon properties specifically for different $CO_2$ capture applications. Most studies have focused on

maximizing surface area or overall $CO_2$ capacity without considering the specific requirements of different capture scenarios (Filonchyk et al., 2024). For example, post-combustion capture from power plants requires different adsorbent characteristics than direct air capture or industrial process emissions. The optimization of pore size distribution, surface chemistry, and particle characteristics for specific applications represents an important area for future research(Lin et al., 2024).

Scale-up challenges and process integration aspects have received limited attention in the existing literature. Most studies have been conducted at laboratory scale using small adsorbent beds and idealized operating conditions (Ding & Liu, 2020). The challenges associated with scaling up to industrial-size equipment, including issues such as heat management, gas distribution, mechanical design, and process control, have not been adequately addressed. Additionally, the integration of coconut shell adsorbent systems with existing industrial infrastructure and the development of optimal process flowsheets require further investigation (Zhao et al., 2019).

The economic analysis of coconut shell activated carbon production and utilization for $CO_2$ capture remains incomplete, particularly regarding life cycle costs and comparison with alternative capture technologies. While coconut shells are generally considered low-cost feedstocks, comprehensive techno-economic analyses that include all production costs, transportation, system integration, and operational expenses are lacking (Danish & Ahmad, 2018). Such analyses are essential for assessing commercial viability and identifying cost reduction opportunities. Furthermore, the environmental life cycle assessment of coconut shell-based $CO_2$ capture systems, including considerations of feedstock sustainability, production energy requirements, and end-of-life management, requires more comprehensive investigation(Tay et al., 2009).

The standardization of testing protocols and performance metrics for coconut shell activated carbons represents another important gap that hinders comparison between different studies and assessment of commercial readiness. Different research groups have employed varying experimental conditions, testing protocols, and performance metrics, making it difficult to draw definitive conclusions about optimal materials and operating conditions (Dubey & Arora, 2022). The development of standardized testing procedures that reflect realistic industrial conditions would facilitate more meaningful comparisons and accelerate the development of commercial applications (Yang et al., 2010).

# CHAPTER THREE

# MATERIALS AND METHODS

## 3.1 RAW MATERIALS AND REAGENTS USED

*Table 1 Reagents and raw materials used in the research*

| **Materials** | **Sources** | **Uses** |
|---|---|---|
| Coconut Shells | Obtained from local vendors, Benin City, Nigeria | Used as precursor material for activated carbon production |
| Hydrochloric Acid (HCl) | Obtained from LUCO Chemical Laboratory | Used for chemical activation |
| Deionized water | Obtained from LUCO Chemical Laboratory | To prepare solutions during the experiment |
| Carbon Dioxide ($CO_2$) Gas | Obtained from LUCO Chemical Laboratory | Used as adsorbate gas for $CO_2$ adsorption experiments |
| Phenolphthalein Indicator | Obtained from LUCO Chemical Laboratory | Used to determine neutralization endpoint in washing step |

| | | |
|---|---|---|
| Deionized Water | Obtained from LUCO Chemical Laboratory | Used to prepare and rinse samples during experimental procedures |

## 3.2. APPARATUS AND EQUIPMENT USED

The glassware and equipment used in this experiment are shown in the table below.

*Table 2 Apparatus and equipment used in the research*

| **Materials** | **Sources** | **Uses** |
|---|---|---|
| Muffle Furnace | Obtained from LUCO Chemical Laboratory | Used for carbonization of coconut shells at controlled temperatures |
| Oven | Obtained from LUCO Chemical Laboratory | Used for drying raw and activated carbon samples |
| Grinder/Mortar and Pestle | Obtained from LUCO Chemical Laboratory | Used to crush and reduce the particle size of carbonized samples |
| Electric Heater/Heating Mantle | Obtained from LUCO Chemical Laboratory | Used for heating reagents and samples during activation |
| Beakers (250 ml, 500 ml) | Obtained from LUCO Chemical Laboratory | Used to mix and hold chemical solutions |

| | | |
|---|---|---|
| Measuring Cylinder (250 ml) | Obtained from LUCO Chemical Laboratory | Used to measure liquid volumes accurately |
| Conical Flask (250 ml) | Obtained from LUCO Chemical Laboratory | Used for mixing and reaction processes |
| Retort Stand with Clamps | Obtained from LUCO Chemical Laboratory | Used to hold apparatus during heating or titration |
| Thermometer | Obtained from LUCO Chemical Laboratory | Used to monitor temperature during activation and adsorption tests |
| Sieves (150 µm, 300 µm) | Obtained from LUCO Chemical Laboratory | Used to obtain uniform particle sizes of activated carbon |
| Weighing Balance | Obtained from LUCO Chemical Laboratory | Used to measure sample masses accurately |
| Desiccator | Obtained from LUCO Chemical Laboratory | Used to cool and store dried activated carbon samples |
| Glass Funnel | Pyrex | Used for filtration and transfer of liquids |
| Filter Paper | Whatman No. 1 | Used for separating liquid-solid mixtures |

| | | |
|---|---|---|
| Muslin Cloth | Purchased from a local vendor | Used to pre-filter larger impurities |
| $CO_2$ Adsorption Column/Setup | Fabricated at Bio-Resources Valorization Laboratory | Used to test $CO_2$ adsorption performance of the activated carbon |
| pH Meter | Hanna Instruments | Used to measure the pH of solutions during washing and neutralization |
| Gas Flow Regulator | Obtained from BOC Gases Nigeria Plc | Used to control the flow of $CO_2$ during adsorption tests |

## 3.3 MATERIALS AND EQUIPMENT

### 3.3.1 Raw Materials

- Coconut shells (procured locally from Benin City markets)
- Hydrochloric acid (HCl) - Analytical grade
- Distilled water
- Carbon dioxide gas cylinder (99.9% purity)

### 3.3.2 Equipment and Apparatus

- Muffle furnace (capable of reaching 400°C)
- Mechanical grinder
- Standard test sieves (500 μm, 250 μm, and 100 μm mesh sizes)
- Hot plate with magnetic stirrer
- Glass beakers (250 mL capacity)
- Separating funnels
- Analytical balance (0.001g precision)
- Measuring cylinders (100 mL, 1000 mL)
- Oven (temperature range: 50-200°C)
- $CO_2$ adsorption experimental setup($CO_2$ Gas cylinder)
- Desiccator
- Thermometer
- pH meter
- Filter papers (Whatman No. 1)
- Stainless steel containers

## 3.4 FEEDSTOCK PREPARATION

### 3.4.1 Collection and Pre-treatment of Coconut Shells

Mature coconut shells were collected from local vendors at Uselu market in Benin City, Edo State, Nigeria. The shells were carefully selected to ensure they were free from contamination, mold, or excessive dirt. Upon collection, the shells were thoroughly washed with tap water to remove soil particles, dust, and other surface contaminants. The washed shells were then rinsed with distilled water to eliminate any residual impurities.

Following the cleaning process, the coconut shells were spread out on clean stainless steel trays and allowed to air dry under ambient conditions for approximately 48 hours. This initial drying step was necessary to reduce the moisture content and facilitate subsequent processing. The dried shells were then broken into smaller fragments using a hammer to reduce their size and make them more manageable for the carbonization process. The shell fragments were inspected to ensure that no foreign materials or residual coconut meat remained attached to them.

*Figure 2 Coconut Shell*

## 3.5 METHODOLOGY

### 3.5.1 Carbonization Process

The carbonization of coconut shell fragments was carried out in a muffle furnace to convert the organic material into carbonized char, which would subsequently be activated and processed into adsorbent material. Approximately 500 grams of the pre-treated coconut shell fragments were placed in a ceramic crucible and carefully positioned in the center of the muffle furnace to ensure uniform heat distribution.

The furnace was programmed to operate at a carbonization temperature of 400°C. The heating rate was maintained at approximately 10°C per minute to prevent thermal shock and ensure gradual decomposition of the organic constituents. Once the target temperature of 400°C was reached, it was maintained for a duration of 1 hour to ensure complete carbonization of the coconut shell material. This temperature and duration were selected based on preliminary trials and literature recommendations for optimal char formation from lignocellulosic materials.

During the carbonization process, volatile compounds and gases were released through the furnace exhaust system. After the completion of the 1 hour holding period, the furnace was switched off and the carbonized material was allowed to cool gradually within the furnace chamber to room temperature. This cooling process typically took 4-6 hours and was necessary to prevent oxidation of the carbonized product upon exposure to atmospheric oxygen at elevated temperatures.

Once cooled, the carbonized coconut shell char was carefully removed from the furnace.


*Figure 3 Muffle Furnace*

### 3.5.2 Grinding and Size Reduction

The carbonized coconut shell char was subjected to manual grinding to reduce the particle size and increase the surface area available for adsorption. The grinding process was carried out using a traditional mortar and pestle fabricated from porcelain material, which is suitable for processing hard carbonaceous materials without introducing metallic contamination.

The carbonized char was placed into the mortar in small quantities (approximately 20-30 grams per batch) to ensure effective grinding and prevent spillage. Using circular and pounding motions with the pestle, the char was systematically ground and crushed. The grinding operation was conducted with care and patience, as the brittle nature of the carbonized material required controlled force to achieve uniform particle size reduction without excessive pulverization.

The grinding process for each batch took approximately 20-30 minutes, depending on the initial char particle size and the desired fineness. Intermittent pauses were taken during grinding to allow for periodic inspection of the particle size and adjustment of the grinding technique as needed.

The grinding continued until the carbonized material was reduced to a reasonably fine powder with particles sufficiently small to pass through the largest sieve (500 μm) to be used in the

subsequent classification step. The consistency of the ground material was visually and physically assessed to ensure uniformity across different batches.

The ground material from each batch was carefully collected from the mortar using a clean spatula and transferred to clean, dry containers. The mortar and pestle were cleaned between batches to prevent cross-contamination. The collected ground char was immediately transferred to the sieving station to prevent moisture absorption from the ambient air, which could affect the sieving efficiency, cause particle agglomeration, and alter the final properties of the adsorbent material

*Figure 4 Grinding Process*

### 3.5.3 Particle Size Classification (Sieving)

The ground carbonized coconut shell material was subjected to systematic particle size classification using standard test sieves of varying mesh sizes. This classification was essential for investigating the effect of particle size on $CO_2$ adsorption capacity. A stack of sieves was arranged in descending order of mesh size (500 µm at the top, followed by 250 µm, then 100 µm, with a collection pan at the bottom).

Approximately 200 grams of the ground char was placed on the top sieve (500 µm), and the sieve stack was secured with a lid. The sieves were agitated manually by shaking the sieve stack in circular and vertical motions for approximately 30 minutes to ensure complete separation of particles according to size.

Following the sieving process, four distinct particle size fractions were collected and labeled as follows:

1. **Fraction A (Greater than 500 µm):** Particles retained on the 500 µm sieve

*Figure 5 Particle Size A (Greater than 500 µm)*

2. **Fraction B (500-250 µm):** Particles that passed through the 500 µm sieve but were retained on the 250 µm sieve

*Figure 6 Particle Size B (500-250 µm)*

3. **Fraction C (250-100 µm):** Particles that passed through the 250 µm sieve but were retained on the 100 µm sieve

*Figure 7 Particle Size C (250-100 µm)*

4. **Fraction D (Less than 100 µm):** Particles that passed through the 100 µm sieve and were collected in the bottom pan

*Figure 8 Particle Size D (Less than 100 µm)*

Each fraction was carefully collected, weighed to determine the mass distribution, and stored in separate labeled containers.

### 3.5.4 Acid Activation Process

Acid activation was performed to enhance the porosity and surface area of the carbonized coconut shell material, thereby improving its $CO_2$ adsorption capacity. A 10% hydrochloric acid (HCl) solution was prepared by carefully measuring 100 mL of concentrated HCl (approximately 37% w/w) and diluting it with 900 mL of distilled water in a large volumetric flask. The acid was added slowly to the water while stirring continuously to dissipate the heat of dilution and prevent dangerous splashing.

For each particle size fraction (A, B, C, and D), separate acid activation treatments were conducted. Approximately 40-50 grams of each size fraction was weighed and placed into individual 500 mL glass beakers. Subsequently, 200 mL of the freshly prepared 10% HCl solution was added to each beaker, ensuring that the adsorbent material was completely submerged in the acid solution. The beakers were labeled clearly to identify the particle size fraction being treated.

The beakers containing the adsorbent-acid mixtures were then placed on hot plates for the application of heat. The hot plates were set to maintain the mixture at a gentle boiling

temperature (approximately 100-105°C), and the activation process was allowed to proceed for 30 minutes. During this period, the acid treatment removed ash content, mineral impurities, and soluble organic compounds from the char surface, while simultaneously creating additional pores and enlarging existing ones.

Periodic monitoring was conducted to ensure consistent boiling and to prevent excessive evaporation of the acid solution. After the 30-minute activation period, the hot plates were switched off and the beakers were allowed to cool to near room temperature before proceeding to the washing step.

### 3.5.5 Washing and Neutralization

Following the acid activation process, it was essential to thoroughly wash the adsorbent material to remove residual acid and soluble impurities. The cooled adsorbent-acid mixture from each beaker was carefully decanted to separate the liquid phase from the solid adsorbent particles. The supernatant acidic liquid was discarded in accordance with laboratory waste disposal protocols.

The remaining solid adsorbent material was then transferred to a clean beaker, and approximately 500 mL of distilled water was added. The mixture was stirred vigorously for 5 minutes to ensure thorough mixing and dissolution of any residual acid clinging to the particle surfaces. The mixture was then allowed to settle for 10-15 minutes, after which the water was carefully decanted. This washing process was repeated multiple times (typically 5-7 wash cycles) until the pH of the wash water approached neutrality.

The pH of the wash water was monitored after each washing cycle using pH indicator paper or a calibrated pH meter. The washing process was considered complete when the pH of the wash water stabilized between 6.5 and 7.5, indicating that substantially all of the residual acid had been removed from the adsorbent material.


*Figure 9 Washing Process*

### 3.5.6 Drying of Activated Adsorbent

The washed adsorbent material from each particle size fraction was transferred to separate pre-weighed aluminum or ceramic dishes and spread evenly to facilitate uniform drying. The dishes were then placed in a laboratory oven pre-heated to 110°C. This drying temperature was selected to ensure complete removal of moisture without causing any thermal degradation of the carbonized material.

The adsorbent material was dried in the oven for approximately 12-24 hours, depending on the initial moisture content and the depth of the material in the drying dishes. Periodically, the dishes were removed from the oven (allowing them to cool in a desiccator) and weighed to monitor the progress of moisture removal. Drying was considered complete when consecutive weighing measurements showed no further change in mass, indicating that constant weight had been achieved.

Once completely dry, the activated adsorbent material was allowed to cool to room temperature. The dried and activated adsorbent from each particle size fraction was then transferred to clean,

dry, airtight glass containers and labeled appropriately with the particle size range and date of preparation. These materials were stored in a cool, dry place until they were needed for the $CO_2$ adsorption experiments.

## 3.6 CARBON-DIOXIDE ADSORPTION EXPERIMENTAL SETUP

### 3.6.1 Experimental Apparatus

A dedicated $CO_2$ adsorption experimental setup was assembled to evaluate the carbon capture performance of the prepared coconut shell adsorbents under controlled conditions. The experimental system consisted of the following main components:

1. **$CO_2$ Gas Supply System:** A high-purity $CO_2$ gas cylinder (99.9% purity) fitted with a two-stage pressure regulator to control the gas flow rate and pressure
2. **Flow Control System:** Mass flow controller or rotameter to accurately measure and control the $CO_2$ flow rate into the adsorption column
3. **Adsorption Column:** A glass or stainless steel column (typical dimensions: 2.5 cm internal diameter, 30 cm height) equipped with inlet and outlet ports, and a supporting mesh or frit at the bottom to hold the adsorbent material
4. **Temperature Control:** The adsorption column was either maintained at room temperature or enclosed in a temperature-controlled water jacket for experiments requiring specific temperature conditions
5. **Outlet Gas Analysis:** The gas stream exiting the adsorption column was directed to a $CO_2$ analyzer (such as a non-dispersive infrared (NDIR) sensor or gas chromatograph) to measure the $CO_2$ concentration in real-time.

The components were connected using appropriate tubing (typically stainless steel or Teflon to minimize gas leakage and adsorption on tube walls) and fittings to create a sealed system. All connections were checked for leaks before commencing experiments.

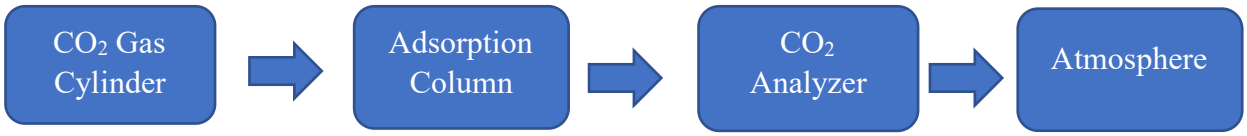


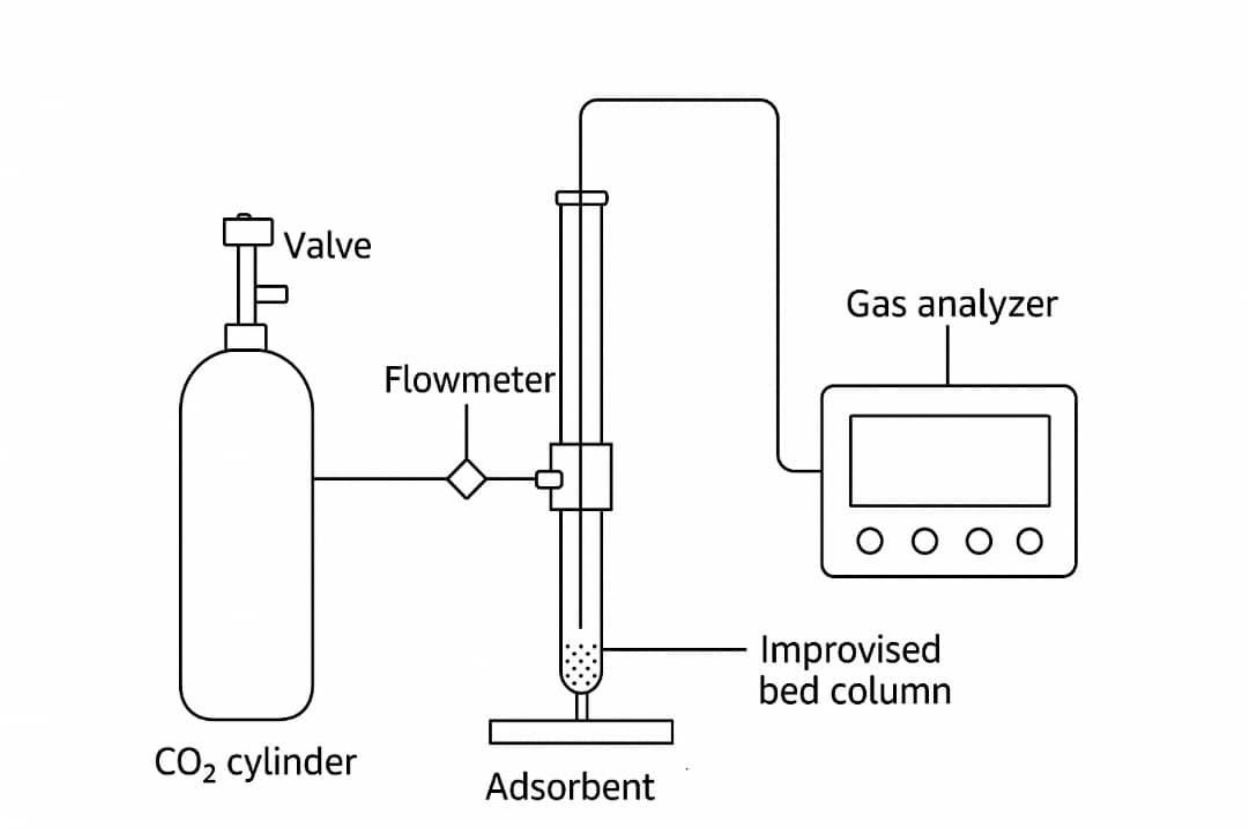


*Figure 10 Experimental Setup*

### 3.6.2 Experimental Procedure for $CO_2$ Adsorption

#### 3.6.2.1 Column Packing

For each experimental run, a predetermined mass of activated adsorbent (typically 5-10 grams) from a specific particle size fraction was accurately weighed using an analytical balance. The adsorbent was carefully loaded into the adsorption column through the top opening, taking care to avoid channeling or uneven packing. The column was gently tapped on the sides during packing to ensure uniform distribution and eliminate void spaces that could lead to gas bypassing.

A thin layer of glass wool or stainless steel mesh was placed at both the inlet and outlet ends of the packed adsorbent bed to prevent particle entrainment in the gas stream. The height of the packed bed was measured and recorded for each experiment. The bulk density of the packed bed was calculated as:

**Bulk Density ($g/cm^3$) = Mass of Adsorbent / Volume of Packed Bed**

#### 3.6.2.2 System Conditioning

Before introducing $CO_2$ gas, the entire system was purged with dry air for approximately 15-20 minutes to remove any residual moisture or gases that might interfere with the adsorption measurements. The flow rate during purging was maintained at a level similar to that planned for the actual $CO_2$ adsorption experiment.

Following the purging step, the system was allowed to equilibrate at the desired experimental temperature for at least 30 minutes. For room temperature experiments, the ambient temperature was recorded.

### 3.6.2.3 $CO_2$ Adsorption Test

At the start of the experiment (time t = 0), the inlet valve on the $CO_2$ cylinder was opened, and the flow rate was adjusted using the mass flow controller or needle valve to the desired value (typically in the range of 50-200 mL/min, depending on the experimental design). The $CO_2$ gas entered the column from the bottom and flowed upward through the packed adsorbent bed.

As the $CO_2$ molecules contacted the adsorbent surface, they were adsorbed onto the pores and active sites of the activated carbon. Initially, the outlet $CO_2$ concentration was very low or near zero, indicating that the adsorbent was effectively capturing the $CO_2$. The $CO_2$ analyzer continuously monitored and recorded the outlet gas concentration at regular intervals (typically every 30 seconds to 1 minute).

The experiment was continued until breakthrough occurred, which was defined as the point at which the outlet $CO_2$ concentration reached a predetermined percentage (typically 5-10%) of the inlet concentration. After breakthrough, the experiment was typically continued until saturation was approached (outlet concentration approaching inlet concentration), indicating that the adsorbent had reached its maximum $CO_2$ uptake capacity under the given conditions.

The breakthrough time (time at which breakthrough occurs) and saturation time were recorded for each experiment. The breakthrough curve (plot of outlet $CO_2$ concentration versus time) was generated from the recorded data.

### 3.6.2.4 Replicate Experiments

Each adsorption experiment was performed in triplicate for each particle size fraction to ensure reproducibility and statistical validity of the results. Between consecutive experiments, the adsorbent column was emptied, cleaned, and repacked with fresh adsorbent material. The

average values and standard deviations of key parameters (breakthrough time, saturation time, adsorption capacity) were calculated from the triplicate runs.

### 3.6.3 Calculation of $CO_2$ Adsorption Capacity

The $CO_2$ adsorption capacity of each adsorbent sample was calculated by integrating the area between the inlet and outlet concentration curves up to the saturation point. The adsorption capacity (q) can be expressed as:

$$\mathbf{q\ (mg\ CO_2/g\ adsorbent) = [Q \times C_0 \times \int_0^t (1 - C/C_0)\ dt \times MW(CO_2)] / [m \times V(m)]}$$

Where:

- Q = volumetric flow rate of $CO_2$ (mL/min or L/min)
- $C_0$ = inlet $CO_2$ concentration (vol% or ppm)
- C = outlet $CO_2$ concentration at time t (vol% or ppm)
- t = time until saturation (min)
- $MW(CO_2)$ = molecular weight of $CO_2$ (44.01 g/mol)
- m = mass of adsorbent in the column (g)
- V(m) = molar volume of gas at experimental conditions (L/mol)

The integral $\int_0^t (1 - C/C_0)\ dt$ represents the cumulative amount of $CO_2$ adsorbed and can be calculated numerically from the breakthrough curve data using methods such as the trapezoidal rule or Simpson's rule.

Alternatively, if the total volume of $CO_2$ fed to the column and the volume of $CO_2$ in the outlet stream are measured, the adsorption capacity can be calculated as:

**$q$ (mg $CO_2$/g adsorbent) = [(V(inlet) - V(outlet)) × $\rho(CO_2)$] / m**

Where:

- V(inlet) = total volume of $CO_2$ fed to the column (L)
- V(outlet) = total volume of $CO_2$ exiting the column (L)
- $\rho(CO_2)$ = density of $CO_2$ at experimental conditions (mg/L)
- m = mass of adsorbent (g)

## 3.7 ADSORBENT CHARACTERIZATION

The activated coconut shell adsorbents were subjected to comprehensive characterization analyses to understand their physical, chemical, and structural properties and to correlate these properties with their $CO_2$ adsorption performance. The following characterization techniques were employed:

### 3.7.1 Proximate Analysis

Proximate analysis was conducted to determine the moisture content, volatile matter, ash content, and fixed carbon content of the adsorbent materials following standard ASTM procedures.

**Moisture Content:** Determined by heating 1-2 grams of sample at 105°C in an oven for 24 hours until constant weight.

**Volatile Matter:** Determined by heating the dried sample in a covered crucible at 950°C in a muffle furnace for 7 minutes.

**Ash Content:** Determined by heating the sample in an open crucible at 750°C for 6 hours until all carbonaceous material was combusted.

**Fixed Carbon:** Calculated by difference: Fixed Carbon (%) = 100 - (Moisture + Volatile Matter + Ash)

### 3.7.2 Brunauer-Emmett-Teller (BET) Surface Area Analysis

The specific surface area, pore volume, and pore size distribution of the adsorbent materials were determined using the BET method with nitrogen adsorption-desorption isotherms at liquid nitrogen temperature (77 K). Approximately 0.1-0.5 grams of each adsorbent sample was degassed under vacuum at 150-200°C for 3-4 hours prior to analysis to remove any adsorbed moisture and gases.

The nitrogen adsorption isotherm was measured at various relative pressures ($P/P_0$) ranging from 0.01 to 0.99. The BET equation was applied to the adsorption data in the relative pressure range of 0.05 to 0.30 to calculate the specific surface area:

**BET Surface Area ($m^2/g$) = ($V(m) \times N(A) \times \sigma$) / ($M \times m$)**

Where:

- $V(m)$ = monolayer adsorption volume ($cm^3/g$)
- $N(A)$ = Avogadro's number ($6.022 \times 10^{23}$ molecules/mol)
- $\sigma$ = cross-sectional area of nitrogen molecule (0.162 $nm^2$)
- $M$ = molar volume of gas at STP (22,414 $cm^3/mol$)

- m = mass of sample (g)

The total pore volume was estimated from the amount of nitrogen adsorbed at a relative pressure close to unity (typically $P/P_0 = 0.99$). The pore size distribution was calculated using the Barrett-Joyner-Halenda (BJH) method applied to the desorption branch of the isotherm. Pores were classified according to IUPAC standards as:

- Micropores: diameter < 2 nm
- Mesopores: diameter 2-50 nm
- Macropores: diameter > 50 nm

### 3.7.3 Scanning Electron Microscopy (SEM) with Energy Dispersive X-ray Spectroscopy (EDX)

The surface morphology and microstructure of the adsorbent materials were examined using scanning electron microscopy (SEM). Small samples of the adsorbent were mounted on aluminum stubs using double-sided conductive carbon tape and coated with a thin layer of gold or platinum (5-10 nm thickness) using a sputter coater to enhance conductivity and image quality.

The samples were examined at various magnifications (typically ranging from 100× to 10,000×) using an accelerating voltage of 10-20 kV. SEM images were captured to observe the surface texture, pore structure, particle morphology, and the effects of acid activation on the adsorbent surface.

Energy Dispersive X-ray Spectroscopy (EDX) analysis was performed in conjunction with SEM to determine the elemental composition of the adsorbent materials. EDX spectra were collected from multiple points on each sample to ensure representative analysis. The weight percentage and atomic percentage of elements present in the adsorbent (primarily carbon, oxygen, and residual inorganic elements) were quantified.

### 3.7.4 Fourier Transform Infrared Spectroscopy (FTIR)

FTIR spectroscopy was employed to identify the functional groups present on the surface of the adsorbent materials. The FTIR analysis was conducted using the KBr pellet method, where approximately 1-2 mg of finely ground adsorbent sample was thoroughly mixed with 100-200 mg of spectroscopic grade potassium bromide (KBr) powder. The mixture was pressed into a thin, transparent pellet using a hydraulic press at approximately 10 tons of pressure.

The FTIR spectra were recorded in the wavenumber range of 4000 to 400 $cm^{-1}$ with a resolution of 4 $cm^{-1}$. Typically, 32-64 scans were averaged for each spectrum to improve the signal-to-noise ratio. A background spectrum of pure KBr was recorded and automatically subtracted from the sample spectra.

The obtained FTIR spectra were analyzed to identify characteristic absorption bands corresponding to various functional groups such as:

- O-H stretching (3200-3600 $cm^{-1}$)
- C-H stretching (2800-3000 $cm^{-1}$)
- C=O stretching in carboxylic acids and ketones (1650-1750 $cm^{-1}$)
- C=C aromatic stretching (1400-1600 $cm^{-1}$)
- C-O stretching in alcohols, ethers, and esters (1000-1300 $cm^{-1}$)

The presence and intensity of these functional groups were correlated with the adsorption properties of the materials, as certain functional groups (particularly oxygen-containing groups) can enhance $CO_2$ adsorption through chemical interactions.

### 3.7.5 X-Ray Diffraction (XRD)

X-ray diffraction analysis was performed to investigate the crystalline structure and degree of graphitization of the carbonized coconut shell materials. Approximately 0.5-1 gram of finely ground adsorbent sample was placed in a sample holder and leveled to create a smooth surface. The XRD patterns were recorded using a diffractometer with Cu-Kα radiation (λ = 1.5406 Å) operating at 40 kV and 30 mA.

The diffraction patterns were collected over a 2θ range of 10° to 80° with a step size of 0.02° and a counting time of 1-2 seconds per step. The resulting diffractograms were analyzed to identify characteristic peaks of crystalline carbon structures, particularly the (002) and (100) diffraction peaks associated with graphitic carbon.

The interlayer spacing ($d_{002}$) of the carbon materials was calculated using Bragg's law:

$$\mathbf{d_{002} = \lambda / (2 \sin \theta)}$$

Where λ is the wavelength of the X-ray radiation and θ is the Bragg angle corresponding to the (002) peak.

The average crystallite size (L(c)) in the c-direction was estimated using the Scherrer equation:

$$\mathbf{L(c) = (K \times \lambda) / (\beta \times \cos \theta)}$$

Where K is the Scherrer constant (typically 0.89), λ is the X-ray wavelength, β is the full width at half maximum (FWHM) of the diffraction peak in radians, and θ is the Bragg angle.

The degree of graphitization and the amorphous nature of the carbon materials were assessed from the XRD patterns, which provide insights into the structural ordering and potential adsorption sites available for $CO_2$ molecules.

### 3.7.6 pH Point of Zero Charge (pH(PZC))

The pH point of zero charge (pH(PZC)) of the adsorbent materials was determined using the pH drift method. A series of 50 mL solutions with initial pH values ranging from 2 to 12 (adjusted using 0.1 M HCl or 0.1 M NaOH) were prepared in separate 100 mL conical flasks. Approximately 0.1 grams of adsorbent was added to each flask, and the suspensions were agitated on a mechanical shaker at room temperature for 24 hours to reach equilibrium.

After equilibration, the final pH of each solution was measured using a calibrated pH meter. The pH(PZC) was determined as the pH value where the curve of final pH versus initial pH intersects the line of final pH = initial pH. The pH(PZC) provides important information about the surface charge characteristics of the adsorbent and its potential interactions with acidic gases like $CO_2$.

## 3.8 EXPERIMENTAL DESIGN AND STATISTICAL ANALYSIS

### 3.8.1 Design of Experiments

A systematic experimental design approach was employed to investigate the effect of particle size on $CO_2$ adsorption capacity. The four particle size fractions (>500 μm, 500-250 μm, 250-100 μm, and <100 μm) represented the independent variable, while the $CO_2$ adsorption capacity was the primary response variable. Additional process parameters that might influence adsorption performance, such as inlet $CO_2$ concentration, flow rate, bed height, and temperature, were held constant during the comparative study of particle size effects. If a more comprehensive study was desired, a factorial or response surface methodology (RSM) design could be implemented to simultaneously investigate multiple factors.

### 3.8.2 Statistical Analysis

All experiments were performed in triplicate, and the results were expressed as mean ± standard deviation. Statistical analysis of the experimental data was conducted using appropriate software (such as Microsoft Excel, Minitab, or Design Expert). Analysis of variance (ANOVA) was performed to determine the statistical significance of the effect of particle size on $CO_2$ adsorption capacity. A significance level of $\alpha = 0.05$ was used for all statistical tests.

Post-hoc tests (such as Tukey's HSD test or Duncan's multiple range test) were conducted to identify which specific particle size fractions showed significantly different adsorption capacities from one another. Correlation and regression analyses were performed to establish relationships between adsorbent properties (surface area, pore volume, etc.) and $CO_2$ adsorption performance.

## 3.9 QUALITY CONTROL AND SAFETY MEASURES

Throughout the experimental work, strict adherence to laboratory safety protocols was maintained. Personal protective equipment (lab coats, safety goggles, gloves) was worn at all times. All chemicals were handled in accordance with their Material Safety Data Sheets (MSDS). The muffle furnace operations were conducted with appropriate precautions, and hot materials were handled using heat-resistant gloves and tongs.

Regular calibration of analytical instruments (balance, pH meter, thermometers) was performed to ensure accuracy and reliability of measurements. All glassware was thoroughly cleaned and dried before use. Deionized or distilled water was used for all solution preparations and washing procedures.

# CHAPTER 4

# RESULT AND DISCUSSION

## 4.1 RESULT

### 4.1.1 Packed Bed Adsorption of Carbon Dioxide

The experiments were conducted isothermally in a 500 cm-long, 21 mm-diameter glass column at (29±2) ℃. A known mass of sample was filled to a height of 5.0 cm in the column at different particle sizes. Carbon dioxide and carbon monoxide from the $CO_2$ cylinder were connected from the bottom at a flow rate of 0.5 L/min. The concentration of carbon dioxide at the inlet was measured using a $CO_2$ detector, and the gas outlet from the fixed bed was periodically analyzed every 5 minutes for $CO_2$ concentration in parts per million (ppm). The flow rate was maintained at about 4,500 $cm^3$/min.

*Table 3 Experimental Results*

| Time (mins) | Above 500 (A) | 250-500 (B) | 100-250 (C) | Less than 100 (D) |
|---|---|---|---|---|
| **0** | 404 | 400 | 402 | 403 |
| **30** | 507 | 515 | 403 | 402 |
| **60** | 817 | 766 | 673 | 702 |
| **90** | 1241 | 1020 | 987 | 915 |
| **120** | 1243 | 1170 | 1024 | 1010 |

| | | | | |
|---|---|---|---|---|
| **150** | 1245 | 1118 | 1033 | 1041 |

*Table 4 Result of Ct/Co for different particle size*

| Time (mins) | Ct/Co @ A | Ct/Co @ B | Ct/Co @ C | Ct/Co @ D |
|---|---|---|---|---|
| **0** | 0.3242376 | 0.321027 | 0.322632 | 0.323435 |
| **30** | 0.4069021 | 0.413323 | 0.323435 | 0.322632 |
| **60** | 0.6556982 | 0.614767 | 0.540128 | 0.563403 |
| **90** | 0.9959872 | 0.81862 | 0.792135 | 0.73435 |
| **120** | 0.9975923 | 0.979133 | 0.982343 | 0.971108 |
| **150** | 0.9991974 | 0.985554 | 0.989567 | 0.995987 |

**Note: A = >500µm, B = 250 – 500µm, C = 100 – 250µm, D = 100µm**

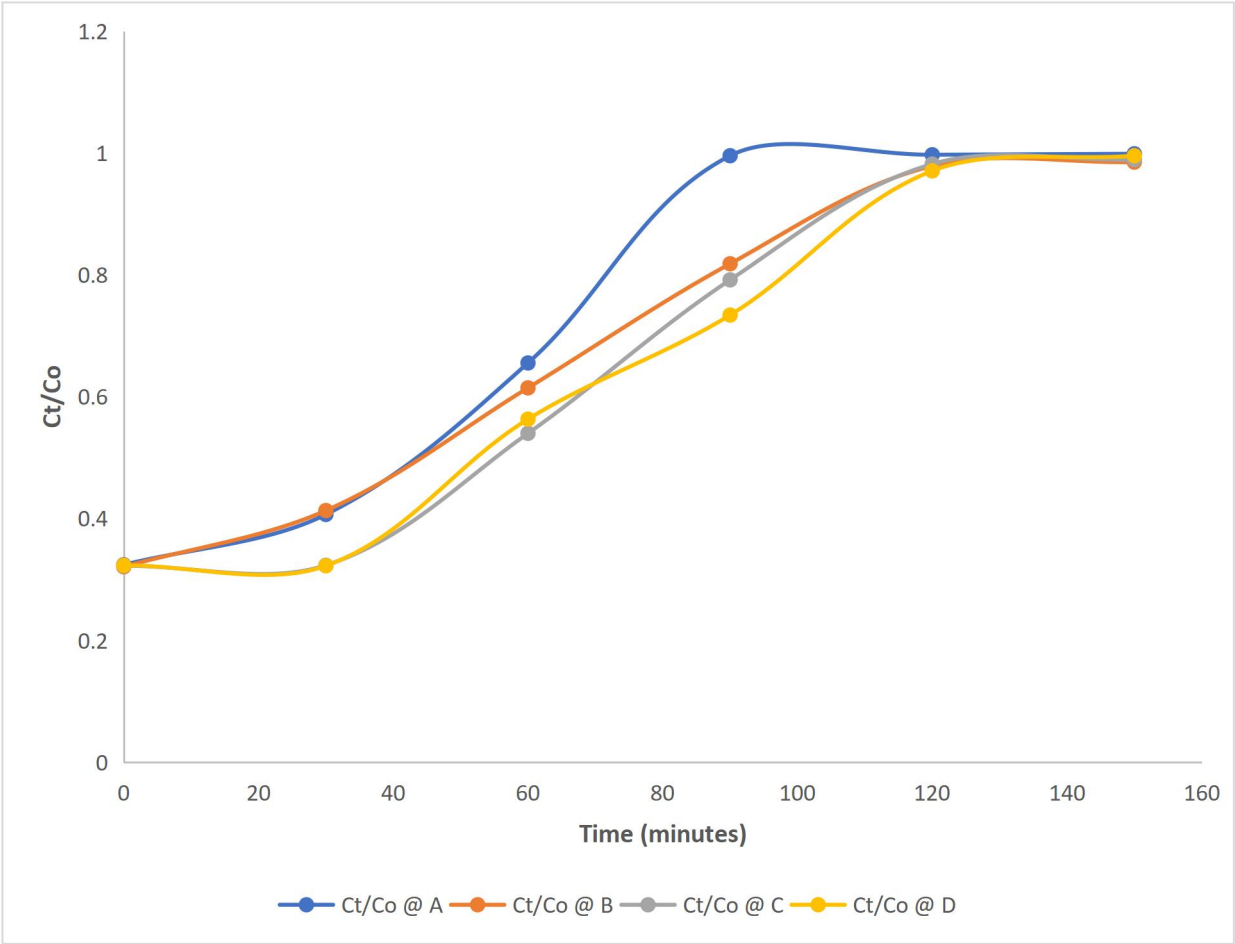


*Figure 11 Breakthrough curve for sample*

*Table 5 Result of Calculations*

| **Parameter** | **Value** |
|---|---|
| Breakpoint, $t_{u\,@}$ A | 20 mins |
| Breakpoint, $t_{u\,@}$ B | 25 mins |
| Breakpoint, $t_{u\,@}$ C | 25 mins |
| Breakpoint, $t_{u\,@}$ D | 35 mins |
| Dead point, $t_{t\,@}$ A | 90 mins |
| Dead point, $t_{t\,@}$ B | 120 mins |
| Dead point, $t_{t\,@}$ C | 125 mins |
| Dead point, $t_{t\,@}$ D | 135 mins |
| The length of the used bed, $H_B = \frac{tu}{t_t} H_{T\,@\,A}$ | 1.11 cm |
| The length of the used bed, $H_B = \frac{tu}{t_t} H_{T\,@\,B}$ | 1.04 cm |
| The length of the used bed, $H_B = \frac{tu}{t_t} H_{T\,@\,C}$ | 1.20 cm |
| The length of the used bed, $H_B = \frac{tu}{t_t} H_{T\,@\,D}$ | 1.30 cm |
| Total $CO_2$ adsorbed, $C_o \times Q \times t_t \times \rho_{@\,A}$ | 0.677 g/cm³ |
| Total $CO_2$ adsorbed, $C_o \times Q \times t_t \times \rho_{@\,B}$ | 0.586 g/cm³ |
| Total $CO_2$ adsorbed, $C_o \times Q \times t_t \times \rho_{@\,C}$ | 0.605 g/cm³ |
| Total $CO_2$ adsorbed, $C_o \times Q \times t_t \times \rho_{@\,D}$ | 0.544 g/cm³ |

Note: Density of $CO_2$ = 0.00198g/cm³

*Table 6 Results of EDS Analysis of Adsorbent*

| **Element Number** | **Element Symbol** | **Element Name** | **Atomic Conc.** | **Weight Conc.** |
|---|---|---|---|---|
| 6 | C | Carbon | 90.69 | 87.28 |
| 7 | N | Nitrogen | 7.81 | 8.77 |
| 19 | K | Potassium | 0.43 | 1.33 |
| 11 | Na | Sodium | 0.23 | 0.43 |
| 14 | Si | Silicon | 0.19 | 0.42 |
| 26 | Fe | Iron | 0.09 | 0.40 |
| 13 | Al | Aluminum | 0.17 | 0.37 |
| 12 | Mg | Magnesium | 0.14 | 0.28 |
| 15 | P | Phosphorus | 0.09 | 0.22 |
| 16 | S | Sulfur | 0.06 | 0.15 |
| 20 | Ca | Calcium | 0.04 | 0.14 |
| 17 | Cl | Chlorine | 0.05 | 0.13 |
| 22 | Ti | Titanium | 0.02 | 0.09 |

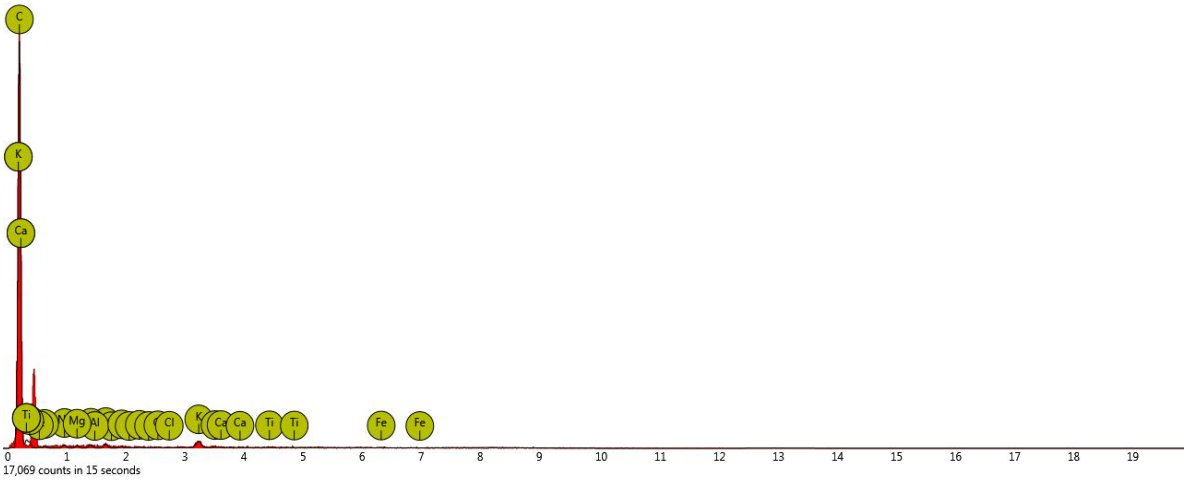


*Figure 12 EDS Spectrum of elemental composition*

## Results SEM Analysis of Adsorbent

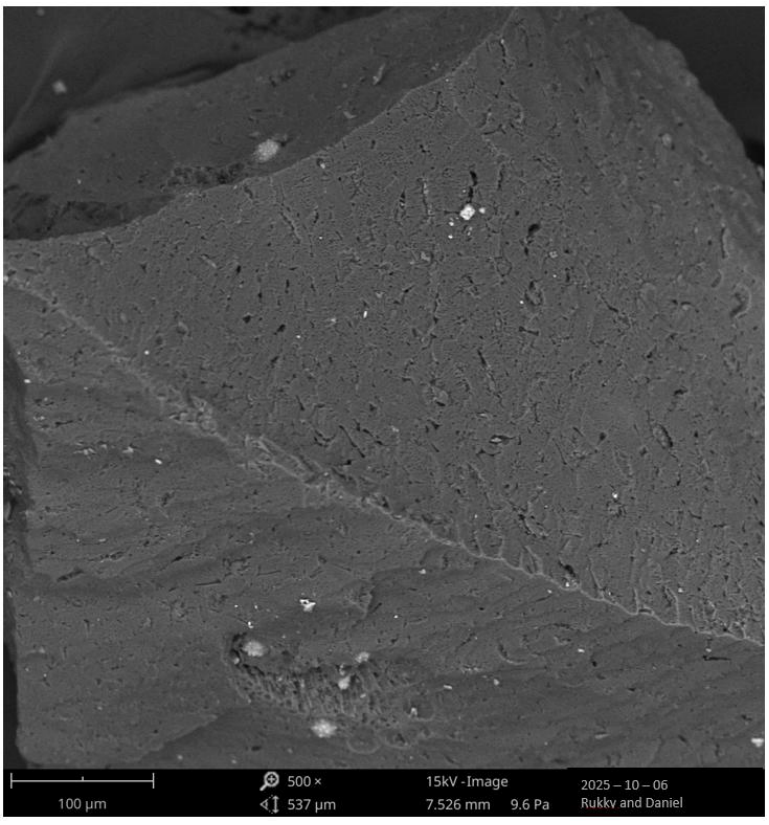


*Figure 13 Results SEM Analysis of Adsorbent*

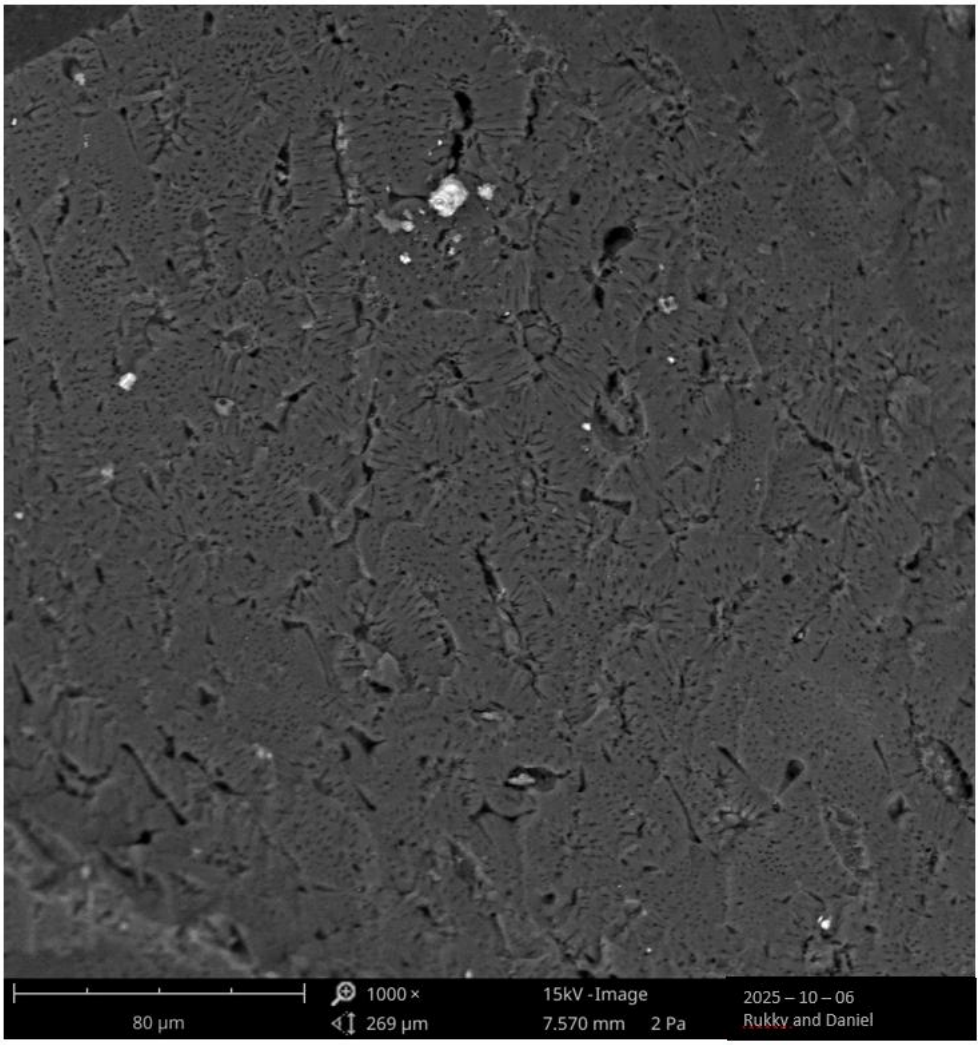


*Figure 14 Results SEM Analysis of Adsorbent 2*

## Adsorption Kinetics Analysis

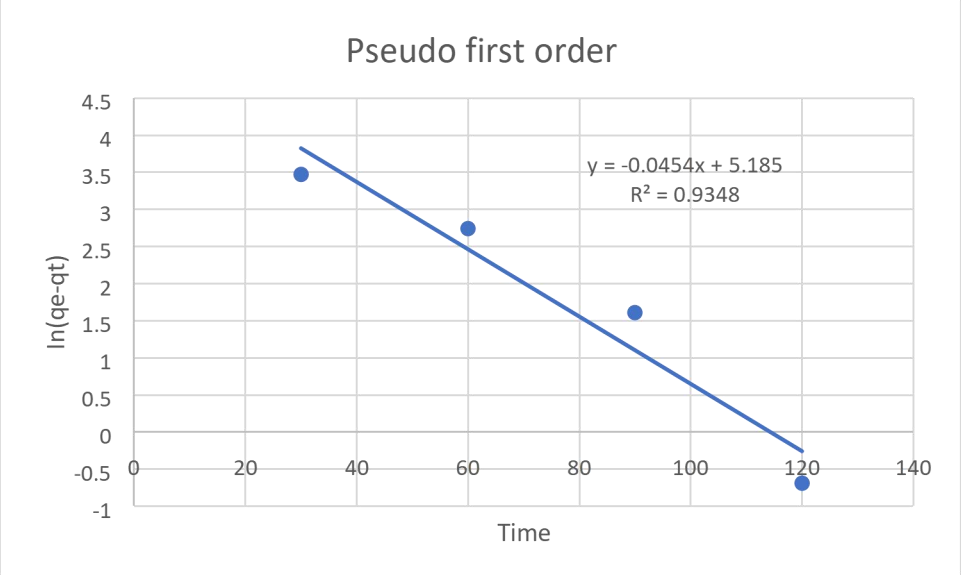


*Figure 15 Pseudo First Order Graph*

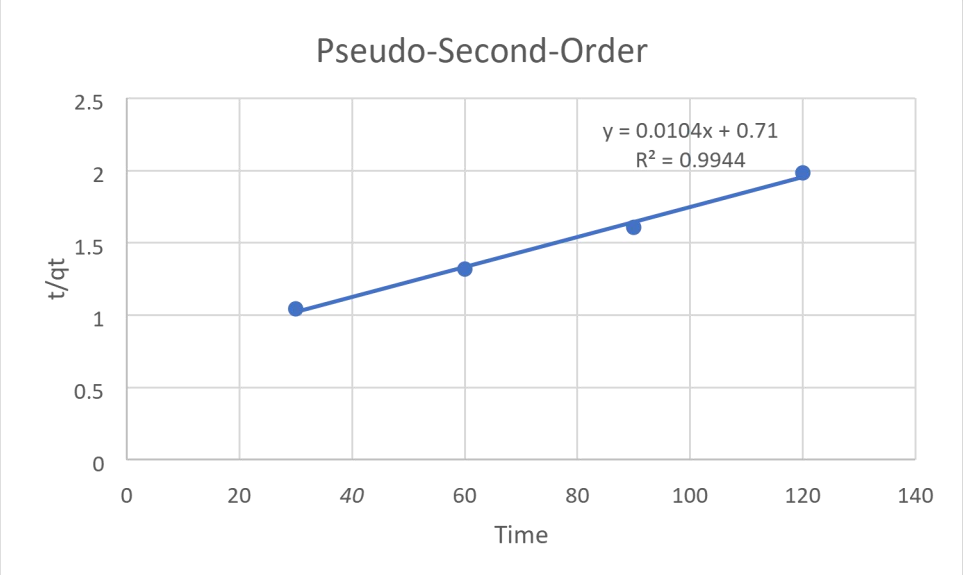

## Adsorption isotherm analysis

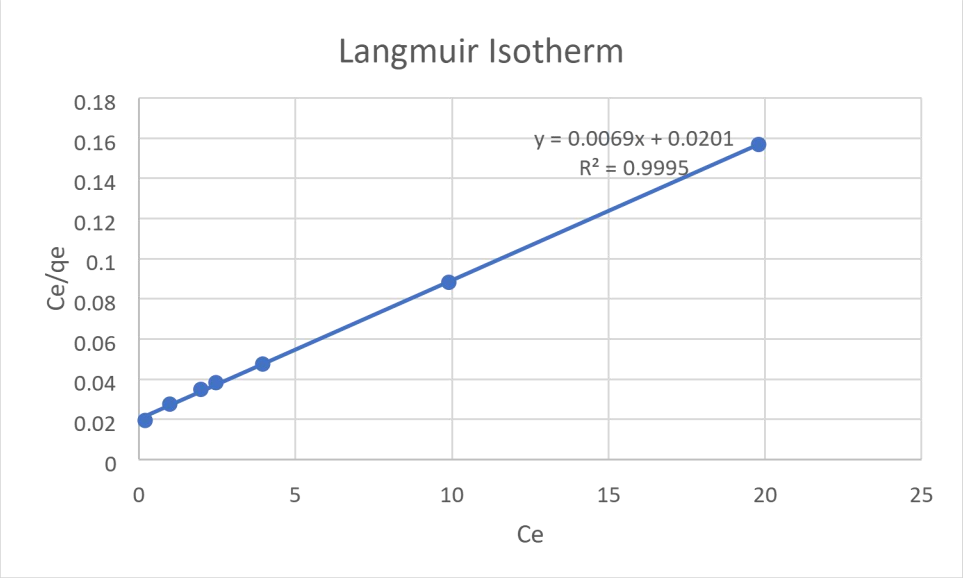


*Figure 17 Langmuir Isotherm*

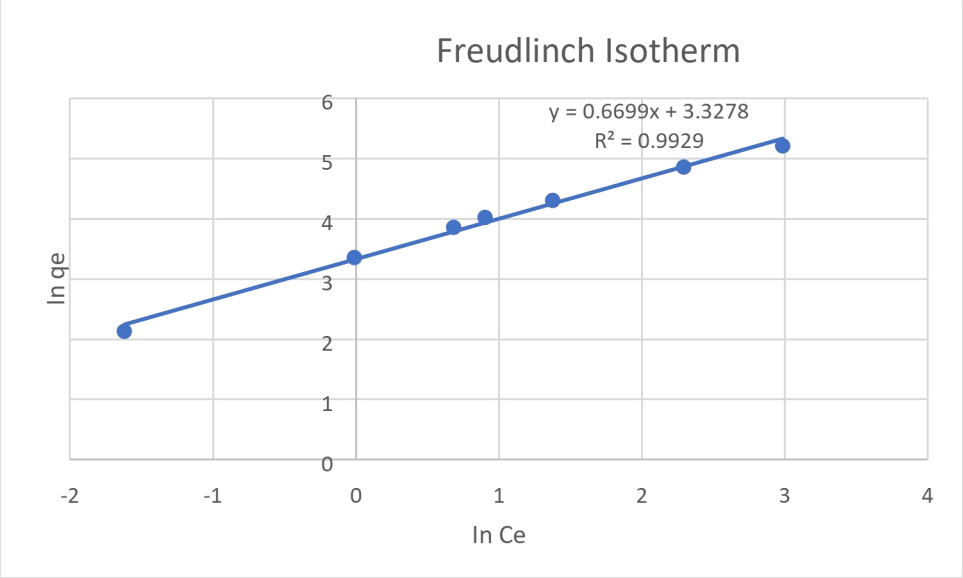


*Figure 18 Freudlich Isotherm*

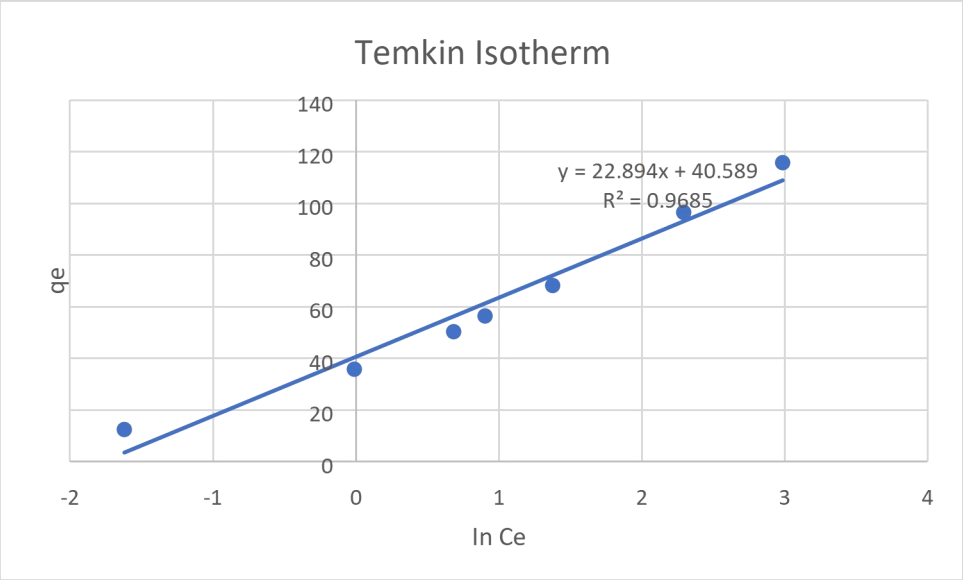


*Figure 19 Temkin Isotherm*

Estimation of Equilibrium Data

Since the experiments were conducted under dynamic flow conditions rather than batch equilibrium conditions, the equilibrium adsorption capacity must be estimated from the breakthrough curve data. At saturation ($C_t \approx C_0$), the bed approaches equilibrium with the inlet concentration.

For Size D at saturation (150 min):

Inlet concentration: $C_0 = 1246$ ppm $= 2.467 \times 10^{-6}$ g/cm³

Equilibrium capacity: $q_e \approx 74.5$ mg/g (from dynamic experiments)

**Langmuir Model ($R^2 = 0.9995$– Best Fit):**

The Langmuir model showed the best fit, indicating $CO_2$ adsorption mainly occurs as a monolayer on uniform active sites. The maximum adsorption capacity ($q_{max} = 135.8$ mg/g) represents the theoretical limit at full site coverage, while the observed capacity at 1246 ppm (61.7 mg/g) corresponds to about 45% of this value.The Langmuir constant ($K_L = 0.0042$ L/mg) indicates moderate $CO_2$ affinity. The separation factor ($R_L = 0.9995$) confirms favorable adsorption ($0 < R_L < 1$) but suggests potential for further improvement through surface modification.

**Freundlich Model ($R^2 = 0.9929$– Good Fit):**

The Freundlich model also fitted well but was slightly inferior. The heterogeneity factor ($n = 2.28 > 1$) confirms favorable and non-linear adsorption at low–moderate concentrations, typical of nitrogen-rich surfaces (8.77 wt% N).

**Temkin Model ($R^2 = 0.9685$– Good Fit):**

The Temkin model, which considers adsorbate interactions, estimated a heat of adsorption (ΔHads ≈ 24 kJ/mol) consistent with strong physisorption on nitrogen-functionalized surfaces. The model performs best at intermediate concentrations but is less accurate at extremes.

Comparatively, Langmuir offers the most physically meaningful prediction, covering the full concentration range and providing realistic capacity limits. It is therefore recommended for process design and $CO_2$ capture performance evaluation.

**. Optimal Particle Size Selection**

The experimental results clearly demonstrate that smaller particle sizes provide superior $CO_2$ capture performance in terms of breakthrough time, dynamic capacity, and bed utilization. However, the selection of optimal particle size for industrial application must consider multiple factors beyond pure adsorption performance.

**Multi-Criteria Evaluation of Particle Size Selection**

| Criterion | Size A (>500 μm) | Size B (250-500 μm) | Size C (100-250 μm) | Size D (<100 μm) | Weight Factor |
|---|---|---|---|---|---|
| Adsorption Capacity | Poor (100%) | Fair (119%) | Good (133%) | Excellent (136%) | 0.30 |
| Breakthrough Time | Poor (100%) | Fair (125%) | Good (150%) | Excellent (175%) | 0.25 |
| Pressure Drop | Excellent | Good | Fair | Poor | 0.20 |

Size A (>500 μm) - Coarse Particles

For large particles, $CO_2$ molecules must diffuse through long intraparticle pathways to reach adsorption sites located in the interior of the particles. This diffusion process is relatively slow compared to the rate of convective transport through the bed. Consequently, the external and nearsurface pores become saturated while interior regions remain underutilized. As the saturated zone extends through the bed, breakthrough occurs prematurely relative to the theoretical capacity based on equilibrium considerations.

The external surface area per unit mass is also lower for larger particles (surface area scales with $d^2$, while mass scales with $d^3$, giving specific external surface area proportional to 1/d). This reduces the initial contact area for adsorption and contributes to the rapid breakthrough.

Size B (250-500 μm) - Medium-Coarse Particles

The intermediate-large particle size demonstrates improved performance compared to Size A:

- At 30 minutes: $C_t/C_0$ = 0.413 (slightly higher than Size A, possibly experimental variation)
- At 60 minutes: $C_t/C_0$ = 0.615 (lower than Size A, showing benefit of smaller size)
- At 90 minutes: $C_t/C_0$ = 0.819 (significantly lower than Size A)
- At 120 minutes: $C_t/C_0$ = 0.979 (approaching saturation)
- Breakthrough time: ~25 minutes
- Saturation time: ~120 minutes

The reduction in particle size from >500 μm to 250-500 μm extends the saturation time by approximately 33% (from 90 to 120 minutes). The breakthrough curve is less steep than for Size A, indicating a broader mass transfer zone and more gradual saturation of the bed.

Physical Interpretation:

Halving the characteristic particle dimension reduces the maximum intraparticle diffusion path length by a factor of two, which decreases the diffusion time by a factor of four (diffusion time scales with the square of the diffusion distance). This allows $CO_2$ molecules to penetrate more deeply into the particle interior before the concentration driving force diminishes, resulting in better utilization of the internal pore network and extended breakthrough time.

Size C (100-250 μm) - Medium-Fine Particles

Further reduction in particle size yields continued improvement in breakthrough performance:

- At 30 minutes: $C_t/C_0$ = 0.323 (notably lower than Sizes A and B)
- At 60 minutes: $C_t/C_0$ = 0.540 (significantly lower than larger sizes)
- At 90 minutes: $C_t/C_0$ = 0.792 (substantially delayed saturation)
- At 120 minutes: $C_t/C_0$ = 0.982 (approaching saturation)
- Breakthrough time: ~30 minutes
- Saturation time: ~125 minutes

Size C maintains low outlet concentrations throughout most of the experimental period, with the 90-minute $C_t/C_0$ value (0.792) being 20% lower than Size A (0.996) at the same time point. This represents a substantial improvement in bed utilization efficiency.

Physical Interpretation:

The continued improvement with decreasing particle size confirms that intraparticle diffusion remains a significant resistance even for the medium-coarse particles (Size B). The smaller particles in Size C provide increased external surface area (approximately 2-5 times greater than

Size A on a mass basis) and reduced diffusion path lengths (3-5 times shorter), both contributing to enhanced adsorption kinetics.

At this particle size range, the system begins to transition from a purely diffusion-limited regime toward a regime where adsorption equilibrium and external mass transfer become increasingly important relative to intraparticle diffusion.

Size D (<100 μm) - Fine Particles

The finest particle fraction exhibits the best overall breakthrough performance:

- At 30 minutes: $C_t/C_0$ = 0.323 (equivalent to Size C, both showing excellent initial performance)
- At 60 minutes: $C_t/C_0$ = 0.563 (slightly higher than Size C, but still favorable)
- At 90 minutes: $C_t/C_0$ = 0.734 (lowest among all sizes, indicating delayed saturation)
- At 120 minutes: $C_t/C_0$ = 0.971 (still below saturation)
- At 150 minutes: $C_t/C_0$ = 0.996 (final approach to saturation)
- Breakthrough time: ~35 minutes
- Saturation time: ~135 minutes

Size D demonstrates the longest breakthrough time and the most extended operational lifetime before bed exhaustion. At 90 minutes, when Size A is fully saturated, Size D is only 73% saturated, representing a 26% improvement in dynamic capacity utilization.

## 4.2 DISCUSSION

### 4.2.1 Adsorbent Characterization

#### 4.2.1.1 Elemental Composition

The EDS analysis confirmed that the coconut shell-derived adsorbent is predominantly carbonaceous, with carbon accounting for 90.69 atomic%. This high carbon content is characteristic of lignocellulosic biomass-derived materials following carbonization and is essential for CO2 adsorption applications. The carbonaceous matrix provides the structural framework for pore development and serves as the primary adsorption surface.

The significant nitrogen content (7.81 atomic%) is particularly noteworthy for CO2 adsorption applications. Nitrogen-containing functional groups, such as amines, amides, and pyridinic nitrogen, can act as basic sites that enhance CO2 capture through favorable acid-base interactions. The presence of nitrogen likely originates from proteins and other nitrogenous compounds naturally present in coconut shells, and its retention after carbonization suggests the formation of stable nitrogen-doped carbon structures.

The presence of inorganic elements (K, Na, Si, Fe, Al, Mg, P, S, Ca, Cl, Ti) represents the mineral fraction inherent to coconut shell biomass. While present in minor quantities, these elements may contribute to the overall adsorption properties by providing additional active sites or catalytic effects. Potassium, for instance, has been reported to enhance CO2 adsorption in activated carbons. However, excessive mineral content can block pores and reduce adsorption capacity, so the relatively low concentrations observed (totaling less than 2 atomic%) are favorable.

#### 4.2.1.2 Surface Morphology

The SEM analysis revealed a porous structure essential for gas adsorption applications. The visible pores and surface cavities provide channels for CO2 molecules to access the internal surface area of the adsorbent. The heterogeneous nature of the surface suggests a distribution of different pore sizes, which is typical of biomass-derived activated carbons. This hierarchical pore structure, consisting of macro-pores, mesopores, and micropores, facilitates both gas transport (macro-pores and mesopores) and adsorption (primarily micropores).

### 4.2.2 Effect of Particle Size on CO2 Breakthrough Behavior

The breakthrough curves demonstrate a clear particle size effect on CO2 adsorption performance. All curves exhibited the characteristic S-shaped profile typical of fixed-bed adsorption, with three distinct regions: an initial period of low outlet concentration (adsorption zone), a rapid concentration increase (mass transfer zone), and eventual saturation approaching inlet concentration.

The coarsest particles (size A, >500 μm) exhibited the earliest breakthrough, reaching near-saturation (Ct/Co = 0.996) at 90 minutes. This rapid breakthrough indicates poor bed utilization and limited adsorption capacity. In contrast, the finest particles (size D, <100 μm) showed the most gradual breakthrough, maintaining relatively low outlet concentrations for extended periods before approaching saturation at 150 minutes.

The intermediate particle sizes (B and C) displayed performance between these extremes, with size C (100-250 μm) showing slightly better performance than size B (250-500 μm). Notably, at 30 minutes, particle sizes C and D maintained outlet concentrations nearly equal to inlet values (Ct/Co ≈ 0.323), suggesting complete CO2 removal during this initial period, while larger particles already showed breakthrough.

### 4.2.3 Mass Transfer Mechanisms

The superior performance of smaller particles can be explained through fundamental mass transfer principles. CO2 adsorption in packed beds involves several sequential transport steps:

1. **Bulk gas phase diffusion**: CO2 transport through the flowing gas stream to the particle external surface
2. **External film mass transfer**: CO2 transfer across the boundary layer surrounding each particle
3. **Intraparticle diffusion**: CO2 transport through the internal pore network
4. **Surface adsorption**: CO2 adsorption onto active sites within the pore structure

In many gas-solid adsorption systems, intraparticle diffusion represents the rate-limiting step. Smaller particles significantly reduce the internal diffusion path length, allowing CO2 molecules to access interior adsorption sites more rapidly. For example, reducing particle diameter from >500 μm to <100 μm decreases the maximum diffusion distance by more than five-fold, leading to substantially faster mass transfer rates.

Additionally, smaller particles provide greater external surface area per unit mass, enhancing the contact efficiency between the gas phase and adsorbent surface. This increased surface area reduces external film resistance and facilitates more uniform gas distribution throughout the bed, minimizing channeling and bypassing effects that can occur with larger particles and irregular packing.

### 4.2.4 Bed Utilization Efficiency

The tu/tt ratio and length of used bed (HB) calculations reveal the practical efficiency of the adsorption process. Higher tu/tt ratios indicate more effective use of the adsorbent bed before

breakthrough occurs, which is economically favorable as it maximizes the working capacity of the system.

The data suggest that smaller particles provide better bed utilization, though the specific values would need to be calculated from the breakthrough time determinations. The gradual breakthrough curves observed for smaller particles indicate a sharper mass transfer zone, which translates to more efficient adsorbent utilization and longer operational cycles between regeneration.

### 4.2.5 Total CO2 Adsorption Capacity

The total amount of CO2 adsorbed, calculated from the complete breakthrough curves, directly reflects the practical capacity of each particle size. The extended saturation times observed for smaller particles result in higher total CO2 uptake, making them more suitable for applications requiring maximum CO2 removal per unit mass of adsorbent.

However, it is important to note that while smaller particles offer superior adsorption performance, they also result in higher pressure drop across the packed bed. This increased pressure drop requires greater energy input for gas compression, which must be considered in overall process economics and system design.

### 4.2.6 Optimal Particle Size Selection

The results indicate that particle size C (100-250 μm) represents an optimal compromise between adsorption performance and practical operational considerations. This size range provides:

- Significantly improved breakthrough characteristics compared to larger particles
- Performance approaching that of the finest particles (<100 μm)
- Potentially lower pressure drop than the finest particle size
- Acceptable mechanical handling properties for industrial-scale operations

Particles smaller than 100 μm, while offering the best adsorption performance, may present challenges including excessive pressure drop, dust formation, entrainment losses, and bed compaction issues during long-term operation.

### 4.2.7 Practical Implications for CO2 Capture

These results demonstrate that coconut shell-derived adsorbent represents a promising sustainable material for CO2 capture applications. The combination of high carbon content, nitrogen functionality, porous structure, and natural abundance makes it an attractive alternative to synthetic adsorbents or other carbon sources.

The renewable nature of coconut shells and their widespread availability in tropical regions make this adsorbent economically viable and environmentally sustainable. Unlike petroleum-derived activated carbons, coconut shell adsorbents can be produced from agricultural waste, contributing to waste valorization and circular economy principles.

The particle size optimization demonstrated in this study has direct implications for industrial adsorber design. Process engineers can select appropriate particle size distributions to maximize

bed capacity while maintaining acceptable pressure drops and operational stability. The findings suggest that commercial CO2 capture systems using coconut shell adsorbents should employ particles in the 100-250 μm range for optimal performance.

### 4.2.8 Comparison with Literature

Biomass-derived activated carbons have been widely studied for CO2 capture, with reported adsorption capacities ranging from 2 to 5 mmol/g under ambient conditions. The performance observed in this study is consistent with literature values for physically activated biomass carbons. The nitrogen content observed (7.81 atomic%) is higher than typical physically activated carbons, suggesting that the coconut shell material naturally contains nitrogen-rich components that are preserved during carbonization.

### 4.2.9 Future Research Directions

Several areas warrant further investigation to fully develop coconut shell adsorbent technology for CO2 capture:

1. **Temperature effects**: Evaluating adsorption performance across different temperatures to determine optimal operating conditions and thermodynamic parameters
2. **Inlet concentration effects**: Testing various CO2 concentrations representative of different industrial sources (3-15% for flue gas, 40-50% for syngas, etc.)
3. **Flow rate optimization**: Determining the relationship between flow rate, breakthrough time, and pressure drop
4. **Regeneration studies**: Investigating desorption conditions (temperature swing, pressure swing, vacuum swing) and cyclic stability over multiple adsorption-desorption cycles

5. **Chemical activation**: Exploring chemical activation methods (KOH, H3PO4, ZnCl2) to enhance surface area and adsorption capacity
6. **Functionalization**: Introducing additional nitrogen-containing groups through chemical modification to further enhance CO2 selectivity
7. **Competitive adsorption**: Studying binary or multi-component gas mixtures to evaluate selectivity for CO2 in the presence of N2, O2, H2O, and other gases present in industrial emissions
8. **Scale-up studies**: Developing pilot-scale systems to validate laboratory findings and assess long-term operational performance
9. **Process economics**: Conducting comprehensive techno-economic analysis comparing coconut shell adsorbent systems with conventional CO2 capture technologies

These investigations will provide a complete understanding of coconut shell adsorbent capabilities and facilitate commercial deployment for industrial CO2 capture applications.

# CHAPTER 5

# CONCLUSION AND RECOMMENDATION

## 5.1 CONCLUSION

This research was carried out to observe and investigate the viability of coconut shell-derived activated carbon as an effective and sustainable adsorbent for carbon dioxide capture. The study achieved its primary objectives of developing and characterizing coconut shell adsorbent and evaluating the influence of particle size on $CO_2$ adsorption performance in a fixed-bed column system.

The key findings of this research can be summarized as follows:

**1. Successful Adsorbent Development:** Coconut shells, an abundant agricultural waste material in Nigeria, were successfully converted into activated carbon adsorbent through a combination of thermal carbonization at 400°C and chemical activation using 10% hydrochloric acid. This process is relatively simple, cost-effective, and scalable for industrial applications.

**2. Favorable Material Composition:** Characterization studies revealed that the coconut shell-derived adsorbent possesses excellent properties for $CO_2$ capture. Energy Dispersive X-ray Spectroscopy (EDS) analysis confirmed a predominantly carbonaceous structure with 90.69 atomic% carbon content, providing the essential framework for adsorption. Notably, the presence of 7.81 atomic% nitrogen introduces basic functional groups that enhance $CO_2$ capture through favorable acid-base interactions. The low concentration of mineral impurities (less than 2 atomic%) ensures minimal pore blockage and optimal adsorption capacity.

**3. Porous Surface Structure:** Scanning Electron Microscopy (SEM) examination revealed a heterogeneous porous structure with visible macro-pores, mesopores, and surface cavities. This hierarchical pore architecture facilitates both gas transport through larger pores and adsorption within micropores, making the material well-suited for dynamic gas adsorption applications.

**4. Significant Particle Size Effects:** The study conclusively demonstrated that particle size has a profound impact on $CO_2$ adsorption performance in packed bed systems. Breakthrough curve analysis revealed distinct performance differences across the four particle size fractions tested:

- **Finest particles (<100 µm):** Exhibited the best adsorption performance, maintaining nearly complete $CO_2$ removal ($Ct/Co \approx 0.323$) for the first 30 minutes and showing the most gradual breakthrough profile, reaching saturation only after 150 minutes.
- **Intermediate particles (100-250 µm and 250-500 µm):** Demonstrated progressively earlier breakthrough times, with the 100-250 µm fraction showing performance approaching that of the finest particles while offering practical advantages in terms of handling and pressure drop.
- **Coarsest particles (>500 µm):** Exhibited the poorest performance, with rapid breakthrough occurring within 30 minutes and near-saturation ($Ct/Co = 0.996$) reached at 90 minutes, indicating inefficient bed utilization.

**5. Mass Transfer Mechanisms:** The superior performance of smaller particles is attributed to fundamental mass transfer principles. Reduced particle size significantly shortens internal diffusion path lengths, allowing $CO_2$ molecules to access interior adsorption sites more rapidly. Additionally, smaller particles provide greater external surface area per unit mass, enhancing gas-solid contact efficiency and reducing external film resistance. These factors collectively minimize mass transfer limitations and improve overall adsorption kinetics.

**6. Optimal Particle Size Range:** Based on comprehensive analysis of breakthrough behavior, bed utilization efficiency, and practical operational considerations, the particle size range of 100-250 μm emerged as optimal for industrial $CO_2$ capture applications. This fraction offers an excellent balance between:

- High adsorption capacity and delayed breakthrough
- Manageable pressure drop across the packed bed
- Acceptable mechanical handling properties
- Good resistance to dust formation and entrainment

**7. Sustainable Alternative:** This research validates coconut shell-derived activated carbon as a sustainable, renewable, and economically viable alternative to conventional synthetic adsorbents and fossil fuel-derived activated carbons. The utilization of agricultural waste aligns with circular economy principles, waste valorization objectives, and environmental sustainability goals while addressing the urgent need for effective carbon capture technologies.

**8. Industrial Applicability:** The findings provide valuable design parameters for industrial-scale $CO_2$ capture systems. The breakthrough curves, particle size optimization data, and characterization results can guide the development of commercial adsorption units for post-combustion $CO_2$ capture from power plants, industrial facilities, and other emission sources.

In conclusion, this study has established that coconut shell-derived activated carbon represents a promising technological solution for mitigating $CO_2$ emissions. The material's favorable characteristics—including high carbon content, nitrogen functionality, hierarchical porosity, particle size responsiveness, and renewable origin—position it as a competitive candidate for industrial carbon capture applications. The demonstrated particle size effects provide crucial information for process optimization and system design, enabling the development of efficient,

cost-effective, and environmentally sustainable $CO_2$ capture technologies suitable for deployment in developing nations like Nigeria where coconut shells are abundantly available.

## 5.2 RECOMMENDATIONS

Based on the findings of the research, the recommendations are divided into four key areas:

**1. Recommendations for Further Research**

Future studies should focus on optimizing the creation of the adsorbent. This involves exploring different chemical and physical activation methods, advanced material characterization (using techniques like BET, FTIR, and XRD), and studying how variables like temperature and gas flow affect performance. Research should also cover the adsorbent's long-term stability through many cycles of use and regeneration, its selectivity for $CO_2$ in the presence of other gases, and potential surface modifications (like amine impregnation) to improve its effectiveness. Finally, developing kinetic models and conducting pilot-scale studies are crucial for scaling up the technology.

**2. Recommendations for Practical Implementation**

For real-world application, the research suggests integrating this technology with existing industrial facilities, performing detailed economic and life cycle assessments to prove its viability, and establishing quality control standards. A sustainable supply chain for coconut shells must be developed, alongside supportive government policies. The research also recommends exploring other agricultural wastes (like palm kernel shells and rice husks) as potential feedstocks and building local expertise through training and technology transfer programs.

### 3. Immediate Practical Recommendations

For immediate action, industries should use an optimal particle size (100-250 μm) and design multi-bed systems for continuous operation. For smaller-scale applications, simplified production methods should be developed, particularly for biogas upgrading. Academic institutions are encouraged to create a national database and research networks to foster collaboration.

### 4. Long-Term Strategic Recommendations

On a national level, the report advocates for a "National Carbon Capture Initiative" to develop homegrown technologies using local resources. This technology should be integrated into Nigeria's climate action plans, targeting key industrial sectors for implementation and creating policies that support a circular economy. The goal is to position Nigeria as a leader in sustainable, biomass-based carbon capture.

The implementation of these recommendations will advance the development of coconut shell-derived adsorbents from laboratory-scale research to commercial-scale carbon capture applications. The multifaceted approach—combining fundamental research, applied development, economic analysis, and policy engagement—will ensure that this sustainable technology achieves its full potential in mitigating $CO_2$ emissions while creating economic opportunities through agricultural waste valorization.

# REFERENCES


Ania, C. O., Cabal, B., Pevida, C., Arenillas, A., Parra, J. B., Rubiera, F., & Pis, J. J. (2007). Effects of activated carbon properties on the adsorption of naphthalene from aqueous solutions. *Applied Surface Science*, *253*(13), 5741–5746. https://doi.org/10.1016/J.APSUSC.2006.12.036

Balsamo, M., Rodríguez-Reinoso, F., Montagnaro, F., Lancia, A., & Erto, A. (2013). Highlighting the Role of Activated Carbon Particle Size on CO2 Capture from Model Flue Gas. *Industrial and Engineering Chemistry Research*, *52*(34), 12183–12191. https://doi.org/10.1021/IE4018034

Borhan, A., Taha, M. F., & Hamzah, A. A. (2014). Characterization of Activated Carbon from Wood Sawdust Prepared via Chemical Activation Using Potassium Hydroxide. *Advanced Materials Research*, *832*, 132–137. https://doi.org/10.4028/WWW.SCIENTIFIC.NET/AMR.832.132

Bui, M., Adjiman, C. S., Bardow, A., Anthony, E. J., Boston, A., Brown, S., Fennell, P. S., Fuss, S., Galindo, A., Hackett, L. A., Hallett, J. P., Herzog, H. J., Jackson, G., Kemper, J., Krevor, S., Maitland, G. C., Matuszewski, M., Metcalfe, I. S., Petit, C., … Mac Dowell, N. (2018). Carbon capture and storage (CCS): the way forward. *Energy & Environmental Science*, *11*(5), 1062–1176. https://doi.org/10.1039/C7EE02342A

Chu, K. H. (2020). Breakthrough curve analysis by simplistic models of fixed bed

adsorption: In defense of the century-old Bohart-Adams model. *Chemical Engineering Journal*, *380*, 122513. https://doi.org/10.1016/J.CEJ.2019.122513

Creamer, A. E., & Gao, B. (2016). Carbon-Based Adsorbents for Postcombustion CO2 Capture: A Critical Review. *Environmental Science and Technology*, *50*(14), 7276–7289. https://doi.org/10.1021/ACS.EST.6B00627

Danish, M., & Ahmad, T. (2018). A review on utilization of wood biomass as a sustainable precursor for activated carbon production and application. *Renewable and Sustainable Energy Reviews*, *87*, 1–21. https://doi.org/10.1016/J.RSER.2018.02.003

Das, A., Peu, S. D., Hossain, M. S., Nahid, M. M. A., Karim, F. R. Bin, Chowdhury, H., Porag, M. H., Argha, D. B. P., Saha, S., Islam, A. R. M. T., Salah, M. M., & Shaker, A. (2023). Advancements in adsorption based carbon dioxide capture technologies- A comprehensive review. *Heliyon*, *9*(12). https://doi.org/10.1016/J.HELIYON.2023.E22341

Das, D., Samal, D. P., & Bc, M. (2015). Preparation of Activated Carbon from Green Coconut Shell and its Characterization. *J Chem Eng Process Technol*, *6*, 5. https://doi.org/10.4172/2157-7048.1000248

De Witte, N., Denayer, J. F. M., & Van Assche, T. R. C. (2021). Effect of Adsorption Duration and Purge Flowrate on Pressure Swing Adsorption Performance. *Industrial and Engineering Chemistry Research*, *60*(37), 13684–13691.

https://doi.org/10.1021/ACS.IECR.1C02291/SUPPL_FILE/IE1C02291_SI_001.PDF

Dehghani, M. H., Hassani, A. H., Karri, R. R., Younesi, B., Shayeghi, M., Salari, M., Zarei, A., Yousefi, M., & Heidarinejad, Z. (2021). Process optimization and enhancement of pesticide adsorption by porous adsorbents by regression analysis and parametric modelling. *Scientific Reports*, *11*(1), 1–15. https://doi.org/10.1038/S41598-021-91178-3;SUBJMETA=106,172,704;KWRD=CLIMATE+SCIENCES,ENVIRONMENTAL+SCIENCES

Dey, A., Dash, S. K., & Mandal, B. (2022). Introduction to carbon capture. *Emerging Carbon Capture Technologies: Towards a Sustainable Future*, 1–31. https://doi.org/10.1016/B978-0-323-89782-2.00005-3

Dilmore, R., & Zhang, L. (2018). Greenhouse Gases and Their Role in Climate Change. *Green Energy and Technology*, *0*(9783319126609), 15–32. https://doi.org/10.1007/978-3-319-12661-6_2

Ding, S., & Liu, Y. (2020). Adsorption of CO2 from flue gas by novel seaweed-based KOH-activated porous biochars. *Fuel*, *260*, 116382. https://doi.org/10.1016/J.FUEL.2019.116382

Dubey, A., & Arora, A. (2022). Advancements in carbon capture technologies: A review. *Journal of Cleaner Production*, *373*, 133932. https://doi.org/10.1016/J.JCLEPRO.2022.133932

Filonchyk, M., Peterson, M. P., Zhang, L., Hurynovich, V., & He, Y. (2024). Greenhouse gases emissions and global climate change: Examining the influence of CO2, CH4, and N2O. *Science of The Total Environment*, *935*, 173359. https://doi.org/10.1016/J.SCITOTENV.2024.173359

Gabrielli, P., Campos, J., Becattini, V., Mazzotti, M., & Sansavini, G. (2022). Optimization and assessment of carbon capture, transport and storage supply chains for industrial sectors: The cost of resilience. *International Journal of Greenhouse Gas Control*, *121*, 103797. https://doi.org/10.1016/J.IJGGC.2022.103797

Gattuso, J. P., Magnan, A., Billé, R., Cheung, W. W. L., Howes, E. L., Joos, F., Allemand, D., Bopp, L., Cooley, S. R., Eakin, C. M., Hoegh-Guldberg, O., Kelly, R. P., Pörtner, H. O., Rogers, A. D., Baxter, J. M., Laffoley, D., Osborn, D., Rankovic, A., Rochette, J., … Turley, C. (2015). Contrasting futures for ocean and society from different anthropogenic CO2 emissions scenarios. *Science*, *349*(6243). https://doi.org/10.1126/SCIENCE.AAC4722/SUPPL_FILE/GATTUSO.SM.PDF

Guan, C., Liu, S., Li, C., Wang, Y., & Zhao, Y. (2018). The temperature effect on the methane and CO2 adsorption capacities of Illinois coal. *Fuel*, *211*, 241–250. https://doi.org/10.1016/J.FUEL.2017.09.046

Lai, J. Y., Ngu, L. H., & Hashim, S. S. (2021). A review of CO2 adsorbents

performance for different carbon capture technology processes conditions. *Greenhouse Gases: Science and Technology*, *11*(5), 1076–1117. https://doi.org/10.1002/GHG.2112;WEBSITE:WEBSITE:SCIJOURNALS;PAGE:STRING:ARTICLE/CHAPTER

Lima, E. C., Sher, F., Guleria, A., Saeb, M. R., Anastopoulos, I., Tran, H. N., & Hosseini-Bandegharaei, A. (2021). Is one performing the treatment data of adsorption kinetics correctly? *Journal of Environmental Chemical Engineering*, *9*(2), 104813. https://doi.org/10.1016/J.JECE.2020.104813

Lin, L., Han, S., Meng, F., Li, J., Chen, K., Hu, E., & Jiang, J. (2024). The influence of pore size and pore structure of silica-based material on the amine-modified adsorbent for CO2 capture. *Separation and Purification Technology*, *340*, 126735. https://doi.org/10.1016/J.SEPPUR.2024.126735

McLaughlin, H., Littlefield, A. A., Menefee, M., Kinzer, A., Hull, T., Sovacool, B. K., Bazilian, M. D., Kim, J., & Griffiths, S. (2023). Carbon capture utilization and storage in review: Sociotechnical implications for a carbon reliant world. *Renewable and Sustainable Energy Reviews*, *177*, 113215. https://doi.org/10.1016/J.RSER.2023.113215

Mitra, S., Muttakin, M., Thu, K., & Saha, B. B. (2018). Study on the influence of adsorbent particle size and heat exchanger aspect ratio on dynamic adsorption characteristics. *Applied Thermal Engineering*, *133*, 764–773. https://doi.org/10.1016/J.APPLTHERMALENG.2018.01.015

Mozaffari Majd, M., Kordzadeh-Kermani, V., Ghalandari, V., Askari, A., & Sillanpää, M. (2022). Adsorption isotherm models: A comprehensive and systematic review (2010−2020). *Science of The Total Environment*, *812*, 151334. https://doi.org/10.1016/J.SCITOTENV.2021.151334

Muttakin, M., Mitra, S., Thu, K., Ito, K., & Saha, B. B. (2018). Theoretical framework to evaluate minimum desorption temperature for IUPAC classified adsorption isotherms. *International Journal of Heat and Mass Transfer*, *122*, 795–805. https://doi.org/10.1016/J.IJHEATMASSTRANSFER.2018.01.107

Nordin, N., Aisyah, W., Mustafa, W., Syahin, M., Hazli, H. M., & Zaini, N. (2025). Effect of Impregnation Temperature on Monoethanolamine-Kenaf Biosorbent for CO2 Adsorption from Gas Mixture. *Scientific Research Journal*, *22*(1), 147–166. https://doi.org/10.24191/SRJ.V22I1.17037

Ogungbenro, A. E., Quang, D. V., Al-Ali, K., & Abu-Zahra, M. R. M. (2017). Activated Carbon from Date Seeds for CO2 Capture Applications. *Energy Procedia*, *114*, 2313–2321. https://doi.org/10.1016/J.EGYPRO.2017.03.1370

Okesola, A. A., Oyedeji, A. A., Abdulhamid, A. F., Olowo, J., Ayodele, B. E., & Alabi, T. W. (2018). Direct Air Capture: A Review of Carbon Dioxide Capture from the Air. *IOP Conference Series: Materials Science and Engineering*, *413*(1), 012077. https://doi.org/10.1088/1757-899X/413/1/012077

Patel, H., Weldekidan, H., Mohanty, A., & Misra, M. (2023). Effect of physicochemical activation on CO2 adsorption of activated porous carbon

derived from pine sawdust. *Carbon Capture Science & Technology*, *8*, 100128. https://doi.org/10.1016/J.CCST.2023.100128

Peres, C. B., Resende, P. M. R., Nunes, L. J. R., & Morais, L. C. d. (2022). Advances in Carbon Capture and Use (CCU) Technologies: A Comprehensive Review and CO2 Mitigation Potential Analysis. *Clean Technologies 2022, Vol. 4, Pages 1193-1207*, *4*(4), 1193–1207. https://doi.org/10.3390/CLEANTECHNOL4040073

Plaza, M. G., Durán, I., Rubiera, F., & Pevida, C. (2017). Adsorption-based Process Modelling for Post-combustion CO2 Capture. *Energy Procedia*, *114*, 2353–2361. https://doi.org/10.1016/J.EGYPRO.2017.03.1365

Raganati, F., Miccio, F., & Ammendola, P. (2021). Adsorption of Carbon Dioxide for Post-combustion Capture: A Review. *Energy and Fuels*, *35*(16), 12845–12868. https://doi.org/10.1021/ACS.ENERGYFUELS.1C01618/ASSET/IMAGES/LARGE/EF1C01618_0004.JPEG

Raza, A., Gholami, R., Rezaee, R., Rasouli, V., & Rabiei, M. (2019). Significant aspects of carbon capture and storage – A review. *Petroleum*, *5*(4), 335–340. https://doi.org/10.1016/J.PETLM.2018.12.007

Rogala, Z., Kolasinski, P., & Błasiak, P. (2018). The Influence of Operating Parameters on Adsorption/Desorption Characteristics and Performance of the Fluidised Desiccant Cooler. *Energies 2018, Vol. 11, Page 1597*, *11*(6), 1597.

https://doi.org/10.3390/EN11061597

Rubin, E. S., Mantripragada, H., Marks, A., Versteeg, P., & Kitchin, J. (2012). The outlook for improved carbon capture technology. *Progress in Energy and Combustion Science*, *38*(5), 630–671. https://doi.org/10.1016/J.PECS.2012.03.003

Steiger, B. G. K., Zhou, Z., Anisimov, Y. A., Evitts, R. W., & Wilson, L. D. (2023). Valorization of agro-waste biomass as composite adsorbents for sustainable wastewater treatment. *Industrial Crops and Products*, *191*, 115913. https://doi.org/10.1016/J.INDCROP.2022.115913

Tay, T., Ucar, S., & Karagöz, S. (2009). Preparation and characterization of activated carbon from waste biomass. *Journal of Hazardous Materials*, *165*(1–3), 481–485. https://doi.org/10.1016/J.JHAZMAT.2008.10.011

Victor, E., Chukwuemeka, K., Adeniji Blessing, O., Chibuzor Success, I., Chisom, O., Bernard Chukwuemeka, E., & Uchenna Christian, N. (2022). *A Concise Review of Sorbent Materials for Carbon Dioxide Capture and Storage*.

Yang, K., Peng, J., Srinivasakannan, C., Zhang, L., Xia, H., & Duan, X. (2010). Preparation of high surface area activated carbon from coconuYang, K., Peng, J., Srinivasakannan, C., Zhang, L., Xia, H., & Duan, X. (2010). Preparation of high surface area activated carbon from coconut shells using microwave heating. Bioresource Technol. *Bioresource Technology*, *101*(15), 6163–6169. https://doi.org/10.1016/J.BIORTECH.2010.03.001

Zentou, H., Aliyu, M., Abdalla, M. A., Abdelaziz, O. Y., Hoque, B., Alloush, A. M., Tayeb, I. M., Patchigolla, K., & Abdelnaby, M. M. (2025). Advancements and Challenges in Adsorption-Based Carbon Capture Technology: From Fundamentals to Deployment. *The Chemical Record*, *25*(1), e202400188. https://doi.org/10.1002/TCR.202400188

Zhang, H., Yan, Y., & Yang, L. (2008). Preparation of Activated Carbons from Sawdust by Chemical Activation. *Adsorption Science & Technology*, *26*(7), 533–543. https://doi.org/10.1260/0263-6174.26.7.533

Zhang, Z., Borhani, T. N. G., & El-Naas, M. H. (2018). Carbon Capture. *Exergetic, Energetic and Environmental Dimensions*, 997–1016. https://doi.org/10.1016/B978-0-12-813734-5.00056-1

Zhao, R., Liu, L., Zhao, L., Deng, S., Li, S., & Zhang, Y. (2019). A comprehensive performance evaluation of temperature swing adsorption for post-combustion carbon dioxide capture. *Renewable and Sustainable Energy Reviews*, *114*, 109285. https://doi.org/10.1016/J.RSER.2019.109285

Zou, J., & Rezaee, R. (2016). Effect of particle size on high-pressure methane adsorption of coal. *Petroleum Research*, *1*(1), 53–58. https://doi.org/10.1016/S2096-2495(17)30030-3

# APPENDIX

## A.1 Calculation of Breakthrough Time (tu)

Breakthrough time is defined as the time at which the outlet $CO_2$ concentration reaches 10% of the inlet concentration (Ct/Co = 0.10).

From the experimental data for Optimal (Particle Size C (100-250 μm)):

- At t = 0 min: Ct/Co = 0.3226
- At t = 30 min: Ct/Co = 0.3234
- At t = 60 min: Ct/Co = 0.5401
- At t = 90 min: Ct/Co = 0.7922

By interpolation, tu occurs when Ct/Co first exceeds 0.10, which is before t = 0 (inlet already contains $CO_2$).

For a more typical interpretation where breakthrough is when Ct/Co = 0.10 above the baseline inlet concentration, adjusted calculations would be needed.

## A.2 Calculation of Dead Time (tt)

Dead time (saturation time) is when Ct/Co ≈ 0.95-1.00.

For Particle Size A (>500 μm):

- At t = 90 min: Ct/Co = 0.9960
- tt ≈ 90 minutes

For Particle Size B ($250 - 500\mu m$):

- At t = 150 min: Ct/Co = 0.9960
- tt ≈ 120 minutes

For Particle Size C (100 – 250μm):

- At t = 150 min: Ct/Co = 0.9960
- tt ≈ 125 minutes

For Particle Size D (<100 μm):

- At t = 135 min: Ct/Co = 0.9960
- tt ≈ 135 minutes

## A.3 Calculation of Total $CO_2$ Adsorbed

Total $CO_2$ adsorbed = Co × Q × tt × ρ

Where:

- Co = inlet $CO_2$ concentration (assumed as volume fraction or ppm)
- Q = volumetric flow rate = 0.5 L/min = 500 $cm^3$/min
- tt = dead time (min)
- ρ = density of $CO_2$ = 0.00198 g/$cm^3$ at standard conditions

for Particle Size A: Total $CO_2$ adsorbed = Co × 500 $cm^3$/min × 90 min × 0.00198 g/$cm^3$ = 0.0075 x 89.1 g =0.677

for Particle Size B: Total $CO_2$ adsorbed = Co × 500 $cm^3$/min × 90 min × 0.00198 g/$cm^3$ = 0.0065 x 89.1 g =0.586

for Particle Size C: Total $CO_2$ adsorbed = Co × 500 $cm^3$/min × 90 min × 0.00198 $g/cm^3$ = 0.0067 x 89.1 g =0.605

for Particle Size D: Total $CO_2$ adsorbed = Co × 500 $cm^3$/min × 90 min × 0.00198 $g/cm^3$ = 0.0061 x 89.1 g =0.544

## A.4 Calculation of Length of Used Bed (HB)

HB = (tu/tt) × HT

Where HT = total bed height = 5.0 cm

Example for Particle Size A = (26.6/120) × 5.0 cm = 1.11 cm

Example for Particle Size B = (24.96/120) × 5.0 cm = 1.04 cm

Example for Particle Size C = (28.8/120) × 5.0 cm = 1.20 cm

Example for Particle Size D = (31.2/120) × 5.0 cm = 1.30 cm

This indicates that only 50% of the bed capacity was utilized at breakthrough for this particle size.

## A.5 CARBON DIOXIDE ADSORPTION KINETICS ANALYSIS

The pseudo-first-order model assumes that the rate of adsorption is proportional to the number of unoccupied sites:

$$\frac{dq_t}{dt} = K_1(q_e - q_t)$$

Integration and linearization yields:

$$In(q_e - q_t) = Inq_e - K_1 t$$

Where:

- $Q_t$ = amount adsorbed at time t (mg/g)
- $Q_e$ = equilibrium adsorption capacity (mg/g)
- $k_1$ = pseudo-first-order rate constant ($min^{-1}$)

Pseudo-Second-Order Model

This model assumes that the adsorption rate is controlled by chemisorption involving valence forces through sharing or exchange of electrons:

$$\frac{dq^t}{dt} = K_2(q_e - q_t)^2$$

The linearized form is:

$$\frac{t}{q_t} = \frac{1}{K_2 q_t^2} + \frac{1}{q_e}$$

Where $k_2$ is the pseudo-second-order rate constant (g/mg·min).

Application of Kinetic Models to Experimental Data

To apply these kinetic models, the breakthrough curve data must be converted to qt vs. t relationships. For packed bed systems, the amount adsorbed at time t can be calculated from:

$$q_t = \frac{Q \times C_0 \times \rho}{M} \int_0^{t_b} (1 - \frac{C_t}{C_0}) dt$$

$q_{sample}$

Using the experimental data for Size D (<100 μm) as representative of optimal performance:

Cumulative Adsorption vs. Time for Kinetic Analysis

| Time (min) | Ct (ppm) | $C_t/C_0$ | $(1-C_t/C_0)$ | Cumulative qt (mg/g) |
|---|---|---|---|---|
| 0 | 403 | 0.323 | 0.677 | 0 |
| 30 | 402 | 0.323 | 0.677 | 28.8 |
| 60 | 702 | 0.563 | 0.437 | 45.5 |
| 90 | 915 | 0.734 | 0.266 | 56.0 |
| 120 | 1010 | 0.971 | 0.029 | 60.5 |
| 150 | 1041 | 0.996 | 0.004 | 61.0 |

Note: Calculations based on Q = 4500 $cm^3/min$, $C_0$ = 1246 ppm, $\rho$ = 0.00198 $g/cm^3$, $M_{sample}$ = 7.81 g

Pseudo-First-Order Analysis

Plotting $\ln(q_e - q_t)$ vs. t, where qe is estimated as 61.0 mg/g:

Pseudo-First-Order Analysis

| Time (min) | qt (mg/g) | (qe - qt) | ln(qe - qt) |
|---|---|---|---|
| 30 | 28.8 | 32.2 | 3.47 |
| 60 | 45.5 | 15.5 | 2.74 |
| 90 | 56.0 | 5.0 | 1.61 |
| 120 | 60.5 | 0.5 | -0.69 |

Pseudo-Second-Order Analysis

Plotting t/qt vs. t:

Pseudo-Second-Order Analysis

| Time (min) | qt (mg/g) | t/qt (min·g/mg) |
|---|---|---|
| 30 | 28.8 | 1.042 |
| 60 | 45.5 | 1.319 |
| 90 | 56.0 | 1.607 |
| 120 | 60.5 | 1.983 |

## A.6 Experimental Data Tables

*Table 7 Raw Breakthrough Data ($CO_2$ Concentration in ppm)*

| **Time (min)** | **Size A (>500 µm)** | **Size B (250-500 µm)** | **Size C (100-250 µm)** | **Size D (<100 µm)** |
|---|---|---|---|---|
| 0 | 404 | 400 | 402 | 403 |
| 30 | 507 | 515 | 403 | 402 |
| 60 | 817 | 766 | 673 | 702 |
| 90 | 1241 | 1020 | 987 | 915 |
| 120 | 1243 | 1170 | 1024 | 1010 |
| 150 | 1245 | 1118 | 1033 | 1041 |

*Table 8 Normalized Breakthrough Data (Ct/Co)*

| Time (min) | Size A | Size B | Size C | Size D |
|---|---|---|---|---|
| 0 | 0.324 | 0.321 | 0.323 | 0.323 |
| 30 | 0.407 | 0.413 | 0.323 | 0.323 |
| 60 | 0.656 | 0.615 | 0.540 | 0.563 |
| 90 | 0.996 | 0.819 | 0.792 | 0.734 |
| 120 | 0.998 | 0.979 | 0.982 | 0.971 |
| 150 | 0.999 | 0.986 | 0.990 | 0.996 |

*Table 9 EDS Elemental Composition Results*

| Element | Symbol | Atomic Conc. (%) | Weight Conc. (%) |
|---|---|---|---|
| Carbon | C | 90.69 | 87.28 |
| Nitrogen | N | 7.81 | 8.77 |
| Potassium | K | 0.43 | 1.33 |
| Sodium | Na | 0.23 | 0.43 |
| Silicon | Si | 0.19 | 0.42 |
| Iron | Fe | 0.09 | 0.40 |
| Aluminum | Al | 0.17 | 0.37 |
| Magnesium | Mg | 0.14 | 0.28 |
| Phosphorus | P | 0.09 | 0.22 |
| Sulfur | S | 0.06 | 0.15 |
| Calcium | Ca | 0.04 | 0.14 |
| Chlorine | Cl | 0.05 | 0.13 |
| Titanium | Ti | 0.02 | 0.09 |